

PHOTOELECTRON SPECTROSCOPIC STUDIES OF
SOME POLYATOMIC MOLECULES

by

JAGJIT, SINGH, SANDHU
M.Sc. Panjab University, Chandigarh, 1964

A THESIS SUBMITTED IN PARTIAL FULFILMENT OF
THE REQUIREMENTS FOR THE DEGREE OF
MASTER OF SCIENCE
in the Department of
CHEMISTRY

We accept this thesis as conforming to the
required standard

THE UNIVERSITY OF BRITISH COLUMBIA

April, 1967

In presenting this thesis in partial fulfilment of the requirements for an advanced degree at the University of British Columbia, I agree that the Library shall make it freely available for reference and study. I further agree that permission for extensive copying of this thesis for scholarly purposes may be granted by the Head of my Department or by his representatives. It is understood that copying or publication of this thesis for financial gain shall not be allowed without my written permission.

Department of Chemistry

The University of British Columbia
Vancouver 8, Canada

Date 11.1. 1967

ABSTRACT

The 584 Å photoelectron spectra from eight polyatomic molecules (CH_3I , CH_3Cl , CH_3Br , CH_3CHO , CH_3COCH_3 , SF_6 , CH_3CN and $\text{C}_2\text{H}_5\text{CN}$) are described and shown to give all the ionization potentials less than 21.21 eV in each case.

The results are interpreted in terms of the electronic structures of these molecules as given by molecular orbital theory. They are compared with results from other sources, and agreements and differences explained.

A brief account of other existing methods used for the determination of ionization potentials with their advantages and disadvantages is given. The major components of the instruments are briefly discussed, and use of a Single-Grid Photoelectron Spectrometer in the detection of fine structure in the photoelectron spectra is pointed out.

ACKNOWLEDGEMENT

The work described in this thesis was done under the supervision of Dr. D. C. Frost to whom I would like to express my sincere appreciation. I would also like to thank Professor C. A. McDowell for his interest in the work.

I wish to express my gratitude to Dr. C. E. Brion, Dr. D. A. Vroom and Mr. G. E. Thomas for their helpful discussions, to the technical staff of the Chemistry Department for their skilful assistance and to Miss Donna Symons for typing the manuscript.

CONTENTS

	<u>Page</u>
ABSTRACT	ii
ACKNOWLEDGEMENT	iii
CHAPTER ONE - INTRODUCTION	1
A. Ionization Potentials	3
1. Introduction	3
2. Adiabatic and Vertical Ionization Potentials	3
3. Determination of ionization potentials	5
a) Optical Spectroscopy	5
b) Electron Impact	6
c) Photoionization	8
d) Photoelectron Spectroscopy	9
B. The Franck-Condon Principle	13
CHAPTER TWO - EXPERIMENTAL	16
A. Introduction	16
B. The Samples used and their handling system	18
C. Photoelectron Spectrometer	22
I. The Photon Source	22
2. The Photo-electron Analyzer	24
3. Operation of the Spectrometer	24
4. Vacuum System	26
CHAPTER THREE - RESULTS AND DISCUSSION	28
1. Methyl Halides	28
2. Acetaldehyde	42
3. Acetone	47

	<u>Page</u>
4. Sulfur Hexafluoride	49
5. Methyl Cyanide	52
6. Ethyl Cyanide	59
CHAPTER FOUR - CONCLUSION	61
REFERENCES	62

LIST OF TABLES

1. The Samples used and their origin	20
2. Origin and purity of Methyl Halides	28
3. Ionization Potentials of Methyl Halides	34
4. $^2E_{3/2} - ^2E_{1/2}$ doublet separations of the Methyl Halides	40
5. Ionization Potentials of Acetaldehyde	45
6. Ionization Potentials of Acetone	49
7. Ionization Potentials of Methyl Cyanide and Ethyl Cyanide.	54

LIST OF FIGURES

1. Potential energy curves	4
2. Comparison of Cylindrical and Spherical Analyzer Results for Hydrogen	12
3. The Franck-Condon Principle	14
4. The Spherical Photoelectron Spectrometer	17
5. Photoelectron Spectrum of Argon obtained (a) with double, (b) with single grid in the energy analyzer	19
6. The Sample Handling and Vacuum System	21
7. A Spherical Grid	23
8. Schematic Diagram of Electron Retarding System	25
9. Photoelectron Spectrum of Methyl Iodide	29
10. Photoelectron Spectrum of Methyl Bromide	30
11. Photoelectron Spectrum of Methyl Chloride	31
12. Electron energy level diagram for the Methyl Halides	32
13. Photoelectron Spectrum of Acetaldehyde	43
14. Photoelectron Spectrum of Acetone	48
15. Photoelectron Spectrum of Sulfur Hexafluoride	51
16. Photoelectron Spectrum of Methyl Cyanide	55
17. Photoelectron Spectrum of Ethyl Cyanide	56
18. Electron energy level diagram for HCN, CH_3CN and $\text{C}_2\text{H}_5\text{CN}$	57

CHAPTER I

INTRODUCTION

Although a large amount of information is available on the inner ionization potentials (I.P.'s) of diatomic molecules, and polyatomic molecules with relatively high degrees of symmetry, similar data are not readily available for unsymmetrical polyatomic molecules.

The ionization of polyatomic molecules with relatively high degrees of symmetry such as methyl halides and benzene can be treated theoretically in somewhat the same fashion as diatomic molecules (1). If, now, one considers larger, unsymmetrical polyatomic molecules such as acetaldehyde, the theoretical considerations applied in the above cases can no longer be employed since the number of electronic and vibrational states of the system is too large.

This thesis is mainly concerned with discussions of ionization potentials obtained by studying the kinetic energy distribution of photoelectrons ejected from polyatomic molecules (both symmetric and unsymmetric) when subjected to 584 \AA (21.21 eV) radiation. In this way the ionization potentials of each of the molecules which lie below 20 eV have been measured.

Besides yielding values for the energy levels of the excited states of the various molecular ions, the present studies are also of interest for the following reason. They provide one way in which molecular orbital theories of the electronic structures of these molecules may be tested. This is because it is known from self-consistent field molecular orbital theories (2,3,4,5), that T. Koopmans' theorem indicates (6) to a good approximation that the

energy of an electron in a given molecular orbital is equal to minus the I.P. referring to the removal of an electron from that orbital; and it follows that once the several I.P.'s of a molecule are known, the energies of the various orbitals are likewise known.

A. Ionization Potentials

1. Introduction

Ionization potentials are one of the most important properties of a molecule, and when available they can shed much light upon its behaviour. The ionization potential of a polyatomic molecule may be used (a), to help determine which orbital in the molecule is the most loosely bound (7,8); (b), to deduce information about bond strengths, bond lengths, bond order, and the distribution of electric charge in the molecule (9); and (c), to provide data for the calculation of electronic wave functions (2,10). It is generally recognized, moreover, that there is a relationship between ionization potential and chemical reactivity. Ionization potentials are thus of both theoretical and practical importance, and it is desirable to have methods for their accurate measurement. Theoretical calculations of ionization potentials are extremely complex even for atoms above helium and in most cases give a very inaccurate value for the I.P.

Several experimental methods have been developed for I.P. measurement. The more important of these are optical spectroscopy, electron and photon impact ionization, and photoelectron spectroscopy.

2. Adiabatic and Vertical Ionization Potentials

Two different values of the ionization potential often have to be considered: (1) The adiabatic I.P., which corresponds to a transition from the zeroth vibrational level of the molecular ground state to that of the ionic ground state. Spectroscopic ionization potentials usually correspond to these 'adiabatic' values, since

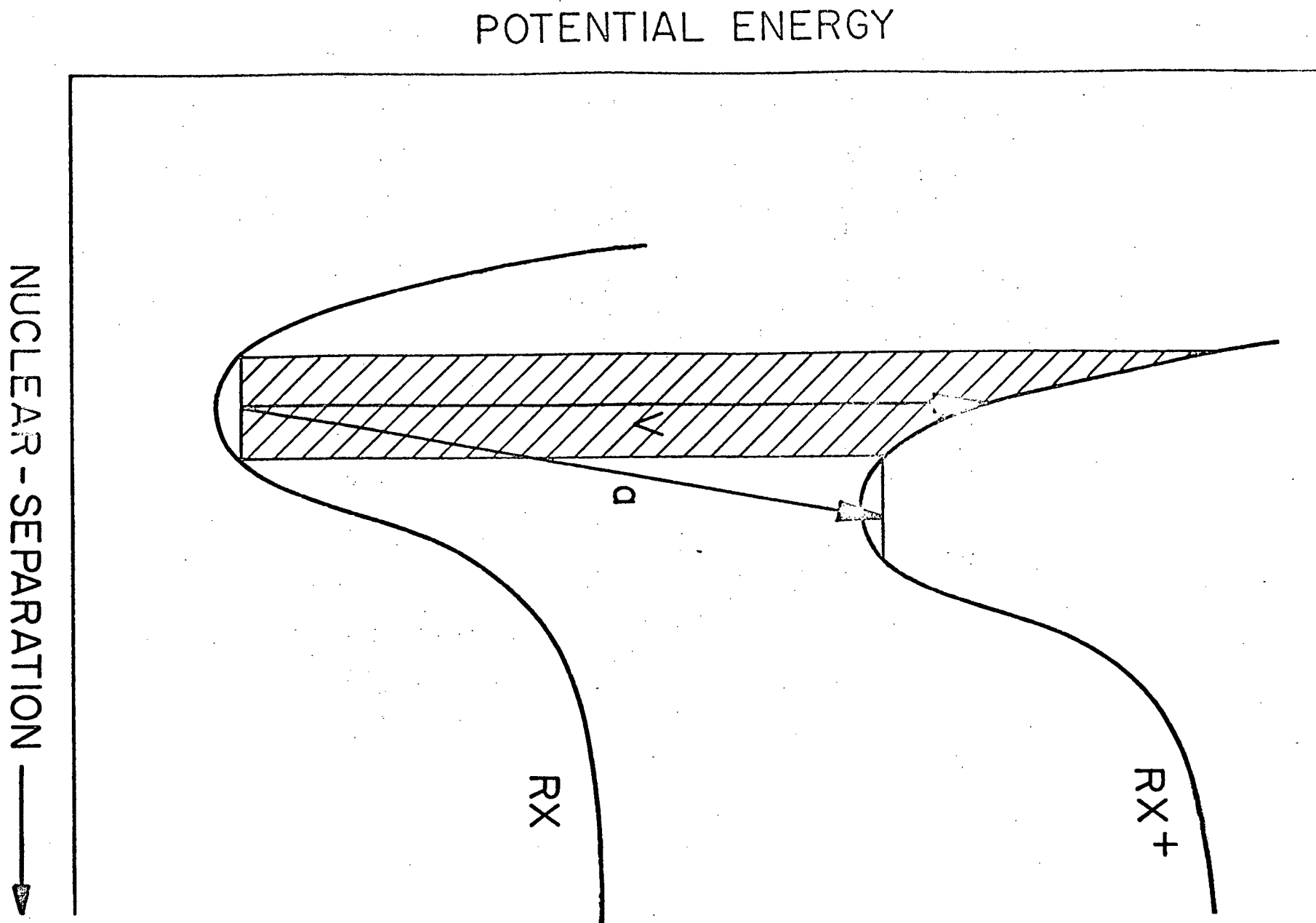


FIGURE 1 Potential Energy Curves.

the 0-0 transition can often be obtained either directly or by extrapolation. The ionization potentials obtained by photoionization are also generally adiabatic.

The vertical I.P. corresponds to the most probable ionization transition from the ground state of the molecule. Ionization potentials measured by electron impact may or may not refer to the ion in its ground vibrational state.

The difference between the adiabatic and vertical potentials can best be illustrated with a diagram, Figure I, where RX is the potential energy curve for the normal electronic state of the molecule, and RX^+ is the potential energy curve for the molecule ion.

It is apparent from Figure I, that the vertical I.P. will usually exceed the adiabatic value because usually there is a difference of r_e between molecule and ion. Experimentally, the difference is usually between 0.02 to 0.5 eV (1).

3. Determination of Ionization Potentials

Various methods have been used for the determination of ionization potentials, and some of them will now be described.

a) The Optical Spectroscopic Method

This method involves the study of that portion of the far-ultraviolet absorption spectrum produced by Rydberg transitions. The most useful form in which to express the Rydberg series is

$$\nu = A - \frac{R}{(n+a)^2}$$

where: A and a are constants for a particular molecule and n takes on integral values representing the different Rydberg bands.

ν = frequency in cm^{-1} of the transition

R = Rydberg constant

This method has been used to obtain accurate values for about 40 molecular ionization potentials. However, it cannot be applied to those molecules which give continuous or diffuse spectra in which it is difficult to deduce the Rydberg convergence limits.

b) The Electron Impact Method

This method uses a heated filament (usually tungsten) as a source of electrons which are passed through the gas under investigation. The intensity of the ions produced is measured as a function of electron energy, and mass analysis is usually employed.

Experimentally, a mixture of the gas under study (for which an ionization potential is desired) and a gas whose ionization potential is known (and will serve as the reference for establishing the energy scale) is subjected to electron bombardment. The inert gases Ar, Kr, etc. are frequently used as standards, since their ionization potentials are known with high accuracy (11). A plot of ion current vs. electron energy provides an "ionization efficiency curve". Now, when one has experimentally found the ionization efficiency curves, the problem becomes one of evaluating these curves to yield the desired I.P. Various techniques have been developed to do this. Nicholson (12) gives an account of eight methods available. It should be noted, however, that all of these

methods are essentially empirical, and even the better ones have definite shortcomings.

The usual mass spectrometer ion source is unsatisfactory for precise ionization studies at low electron energies because of the large spread in electron energies in the beam (13). The other major sources of difficulty are (a) the acceleration of the electrons by an unknown contact potential difference between the cathode and the ionization chamber and (b) an unknown acceleration of the electrons in their passage through the ionization chamber because of the presence of the electric field necessary to extract the ions.

The effect of the electron energy distribution is to obscure fine structure in the ionization efficiency curve. One solution to the problem of resolving the fine structure which may be present in these curves is to reduce the energy spread of the ionizing electron beam.

The two most widely used methods for reducing the energy spread of electron beams are electron velocity selection (14,15) and the Retarding-Potential-Difference (RPD) method (16). Preliminary studies, using the electron energy selector indicate that the $^2P_{3/2}$ and $^2P_{1/2}$ components of the Ar^+ ground state doublet can be resolved. More recent studies on hydrogen show that fine structure is clearly present on the ionization efficiency curve for the H_2^+ ion. This is attributed to the formation of the ion in its various excited vibrational states. Recently mass spectrometric studies of the rare gases using an electron velocity selector (17) have revealed interesting structure in the curves for Kr^+ and Ar^+ . Using the

R.P.D. technique Hickam and coworkers (18) and Frost and McDowell (19) were able to detect the higher excited states of N_2^+ and other ions (20, 21).

Electron impact methods suffer from the defect that in the ionization efficiency curves produced by this method structure is sometimes observed at energies which do not correspond to the known excited states of the ion. Fox and Hickam (22), (in 1954), suggested that such structure in their electron-impact curves was due to auto-ionization (the same as pre-ionization) of a highly excited neutral state of the atom or molecule concerned, and that this phenomenon is of widespread occurrence. Strong evidence in support of their suggestion comes from the photoionization curves for many diatomic molecules, where pre-ionization is clearly indicated.

c) Photoionization

Most of the work in this field has been done by using a monochromator to provide a beam of photons of known narrow energy spread. A gas to be studied is irradiated by these photons, and the resulting photoion current measured as a function of photon energy (23, 24). The first ionization potentials of more than a hundred molecules have recently been reported by Watanabe (25) using this technique, and his results are probably the most accurate to date (since he finds excellent agreement with spectroscopic values where these are available). This method has, however some drawbacks (26), the most serious of which is that because of the lack of mass analysis one has to be sure that the sample being studied is quite free of impurities with lower ionization potentials. Fragment ion formation may also interfere with the "parent" photoion curve.

This difficulty can be overcome by combining the photo-ionization source with a mass spectrometer. This technique has been used by several workers (27, 28, 29) to obtain the first and the inner ionization potentials of several molecules. The main advantage of the method is that it is very much easier to obtain a beam of ultraviolet radiation with a narrow energy spread, and of accurately known energy, than an electron beam with similar properties. Secondly, one does not need a calibrating gas to be introduced along with the sample in order to calibrate the energy scale.

A disadvantage of the photoionization method is that often it becomes difficult to detect inner ionization potentials owing to the structure indicating them being obscured by pre-ionization peaks.

d) Photoelectron Spectroscopy

Although widely used in the determination of work functions of solids, photoelectron spectroscopy has only recently been applied to the study of the I.P.'s of molecules in the gas phase. It enables the direct measurement of all the ionization potentials of a molecule smaller than the value of the ionizing radiation (in our case 21.21 eV). The method was first developed by Vilesov, Kurbatov and Terenin (30), who used a Lozier-type apparatus combined with a vacuum ultraviolet monochromator to measure the kinetic energies of photo-electrons produced on ionization. In 1962, Turner and Al-Joboury (31,32) reported a new method, for the measurement of kinetic energy of photo-ejected electrons which employs the helium resonance line (584 \AA) as the excitation source. Schoen (33), in 1962 started

similar studies using a Seya-Namioka monochromator; but without the disadvantage of optical windows that the Vilesov et al instrument had.

The principle of the method is that a photon of energy $h\nu$ causes the emission of a photo-electron of kinetic energy given very closely by $(h\nu - \text{I.P.})$. Conservation of momentum results in energy partition between the electron and the ion in the inverse ratio of their masses; in the least favourable case (H_2) the mass ratio is 10^4 to 1 and thus the error in equating the electron energy with $(h\nu - \text{I.P.})$ is 1 part in 10^4 ; for larger ions the error is correspondingly less. Virtually all the excess energy is therefore carried away by the photoelectron, so one can write

$$\text{K.E} = h\nu - \text{I.P.} \quad (1-1)$$

where h = Planck's constant

ν = frequency of radiation

I.P. = Ionization potential of the atom or molecule.

It follows that if a gas is irradiated by a monochromatic photon beam there will result as many groups of photoelectrons as the ion has energy levels attainable through absorption of an incident 21.21 eV photon. Kinetic energy measurements will enable the I.P. in each case to be deduced from equation (1-1), and the relative group intensities will be proportional to the relative transition probabilities to the appropriate ionic states. Electron kinetic energies may conveniently be determined by using retarding potential techniques. The plot of the photo-electron intensity as a function of retarding voltage gives the 'integrated' photoelectron spectrum,

which is usually found to consist of series of steps when a spherical analyzer is employed.

In this technique we are thus examining a process or processes occurring in the ionization continua. The important difference from the Rydberg series convergence method, the photoion current method of Watanabe, and from mass spectrometric appearance potential measurements using electron impact is that photoelectron spectroscopy is not a threshold technique. It will usually be free from the limitations imposed by autoionization processes which frequently render higher ionization limits diffuse or unobservable by other methods. However, one does have to use a calibrating gas (Ar, Kr) in order to calibrate the energy scale.

The Instrument used in this work.

In this work a spherical grid analyzer is used to measure the kinetic energy distribution of photoelectrons produced by the interaction of 584 \AA radiation with gas molecules, an arrangement differing significantly from other existing instruments. With spherical grids the electron retarding field is always parallel to the electron trajectory, and this results in a definite increase in resolution, (as shown in Figure 2), over instruments with conventional cylindrical grids (30, 31, 33).

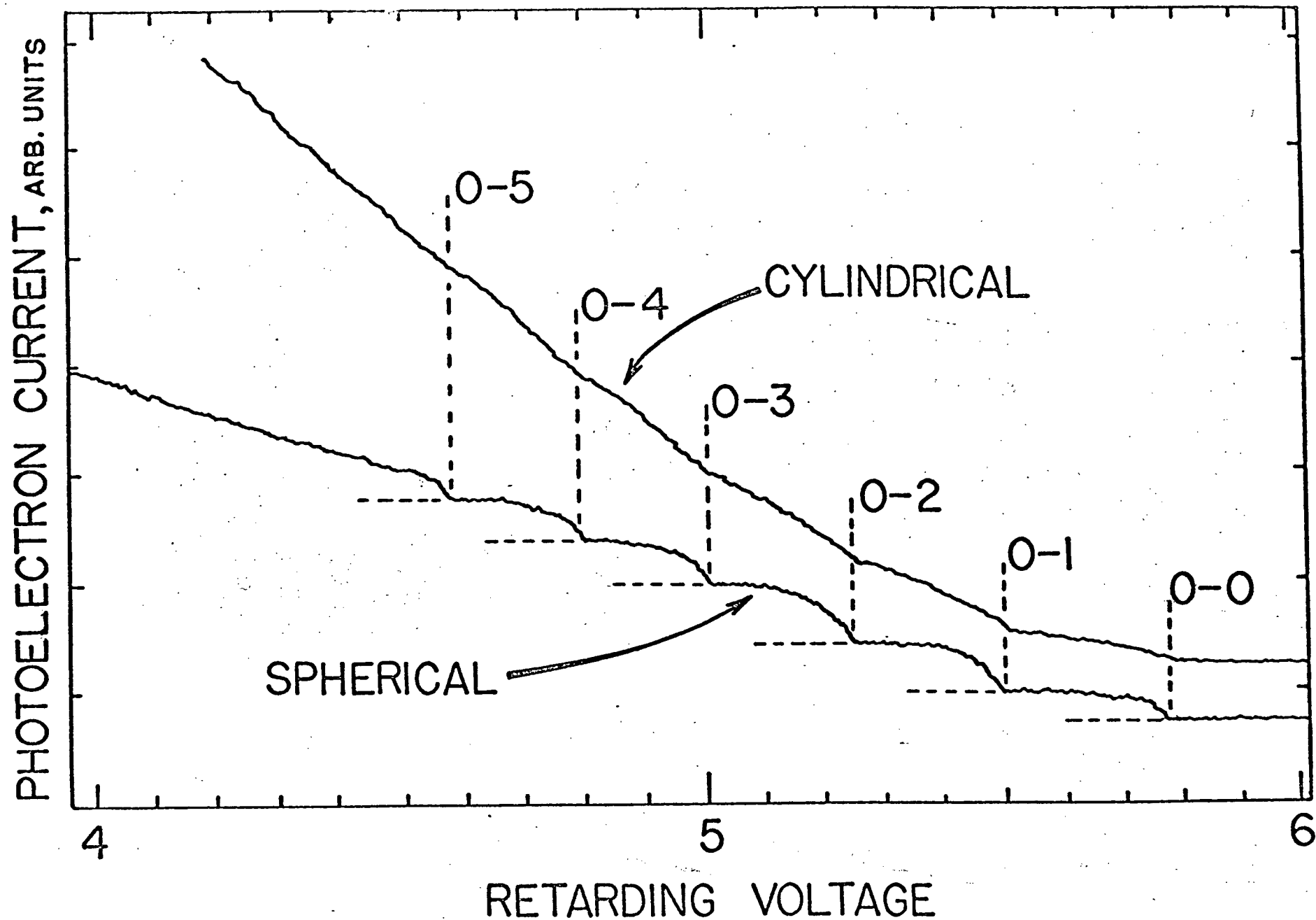


Figure 2 Comparison of Cylindrical and Spherical Analyzer Results for Hydrogen.

B. The Franck-Condon Principle (34, 35)

As pointed out earlier, transitions induced by photon and electron impact obey the Franck-Condon Principle. The principle states that an electronic transition within a molecule takes place so rapidly in comparison to the vibrational motion that immediately afterwards the nuclei still have very nearly the same relative position and velocity as before the "jump". In order to apply this principle to ionization phenomena let us consider Figure 3, in which are drawn the potential energy curves for a diatomic molecule AB in its ground electronic and various ionic excited states.

Figure 3 (a) represents a case where the interatomic distance is the same for the molecular ion and the neutral molecule; in this case the appearance potential will equal the adiabatic I.P. In this case the most probable transition will be to the lowest vibrational level of the ionic state, with very low probability to the higher levels. This gives rise to a single sharp step in the photoelectron energy spectrum, indicating the removal of a non-bonding electron.

When the interatomic distances for the two states differ appreciably, as depicted in Figure 3 (b), it is to be expected that some of the transitions will lead to vibrationally excited AB^+ ions, and others will lead to dissociation of the AB^+ ion to give $(\dot{A} + B$ or $A + B^+$, etc. depending on the limit of the potential energy curve of the upper electronic state at infinite internuclear separation). This will lead to a photoelectron retarding curve exhibiting a great deal of vibrational structure, and then a continuous rise to perhaps above the dissociation limit.

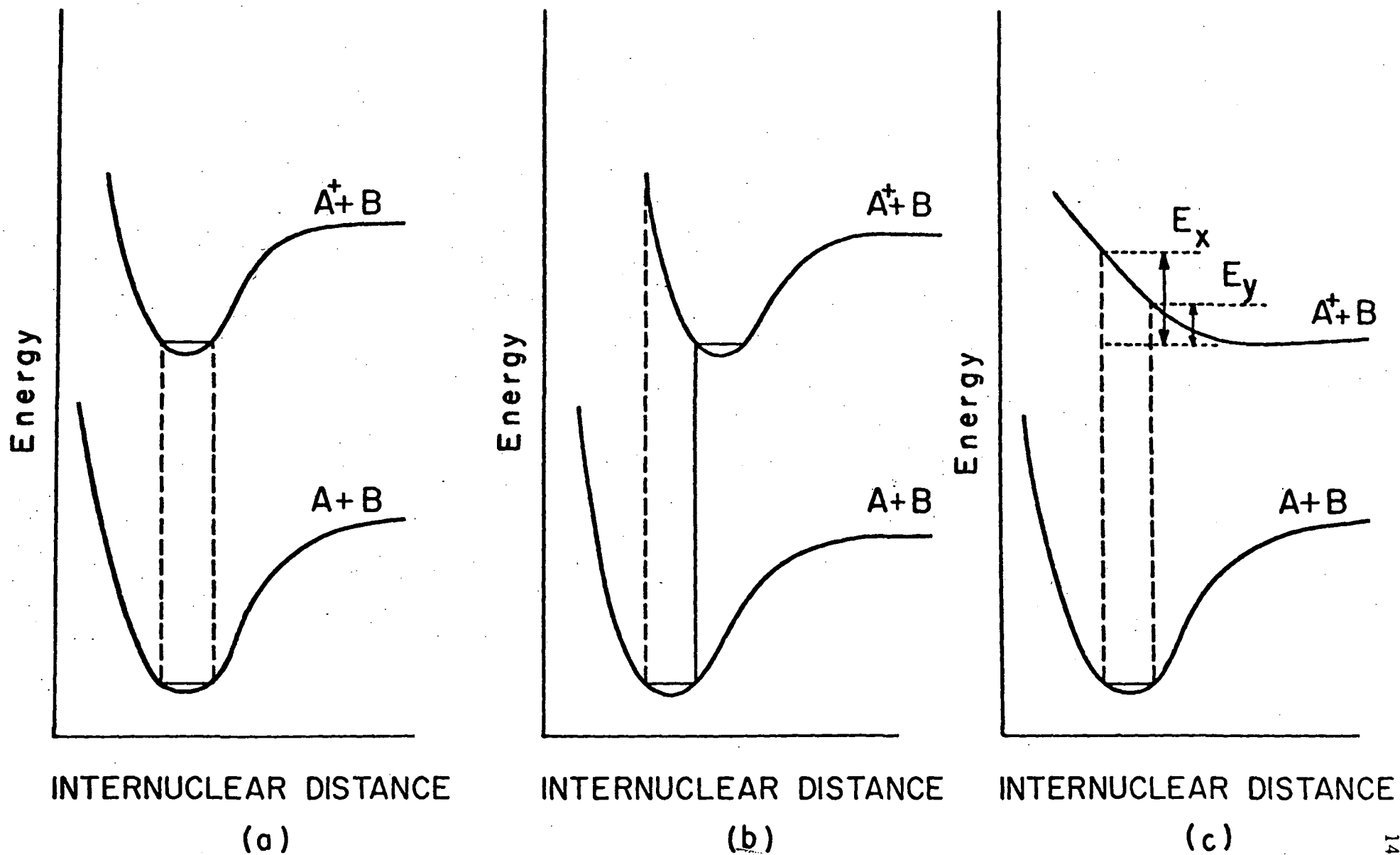


Figure 3 The Franck-Condon Principle

If the upper curve is repulsive, as in Figure 3 (c), then the transitions are no longer to discrete vibrational levels but to a continuum. They will result in dissociation of the molecule ion AB^+ . In such a case, the relative kinetic energies of the fragments (A^+ and B in this example) will have some distribution lying between E_y and E_x .

The electronic transition probability is proportional to the square of the vibrational overlap integral (the integral over the product of the vibrational wavefunctions of the two states involved), when the variation of electronic perturbation integrals with internuclear separation is small (36, 37). Recent work by Nicholls (38) and others has been concerned with the calculation of these Franck-Condon factors for polyatomic as well as diatomic molecules.

CHAPTER II

EXPERIMENTAL

A. Introduction

The photoelectron spectrometer used in this work has been fully described previously (39), and is shown schematically in Figure 4. Only a brief description is given here.

The major advantage the present spectrometer has over others of its type is that it has a spherical grid energy analyzer. All the previous work reported in this field has been done using cylindrical-grid energy analyzers. In these systems electron collection is most efficient for those ejected at 90° to the photon beam and so the collector current is very sensitive to the angular distribution of the photoelectrons. This distribution is roughly a function of $\sin^2 \theta$ (40), where θ is the angle between photon beam and ejected photoelectron trajectory.

These difficulties are overcome in the spherical analyzer used in this work, wherein photoelectrons are produced in a small volume at the centre of the spherical grid system, so that ejection is always normal to the retarding field. This gives rise to greatly improved resolution owing to the 'stepped' photoelectron stopping curve.

One important modification was made during these studies. Previously, the spherical grids were made of brass mesh (30 x 30 mesh 0.005 inch gauge brass) which was gold plated after etching. In this work, new grids constructed from stainless steel mesh (50 by 0.003

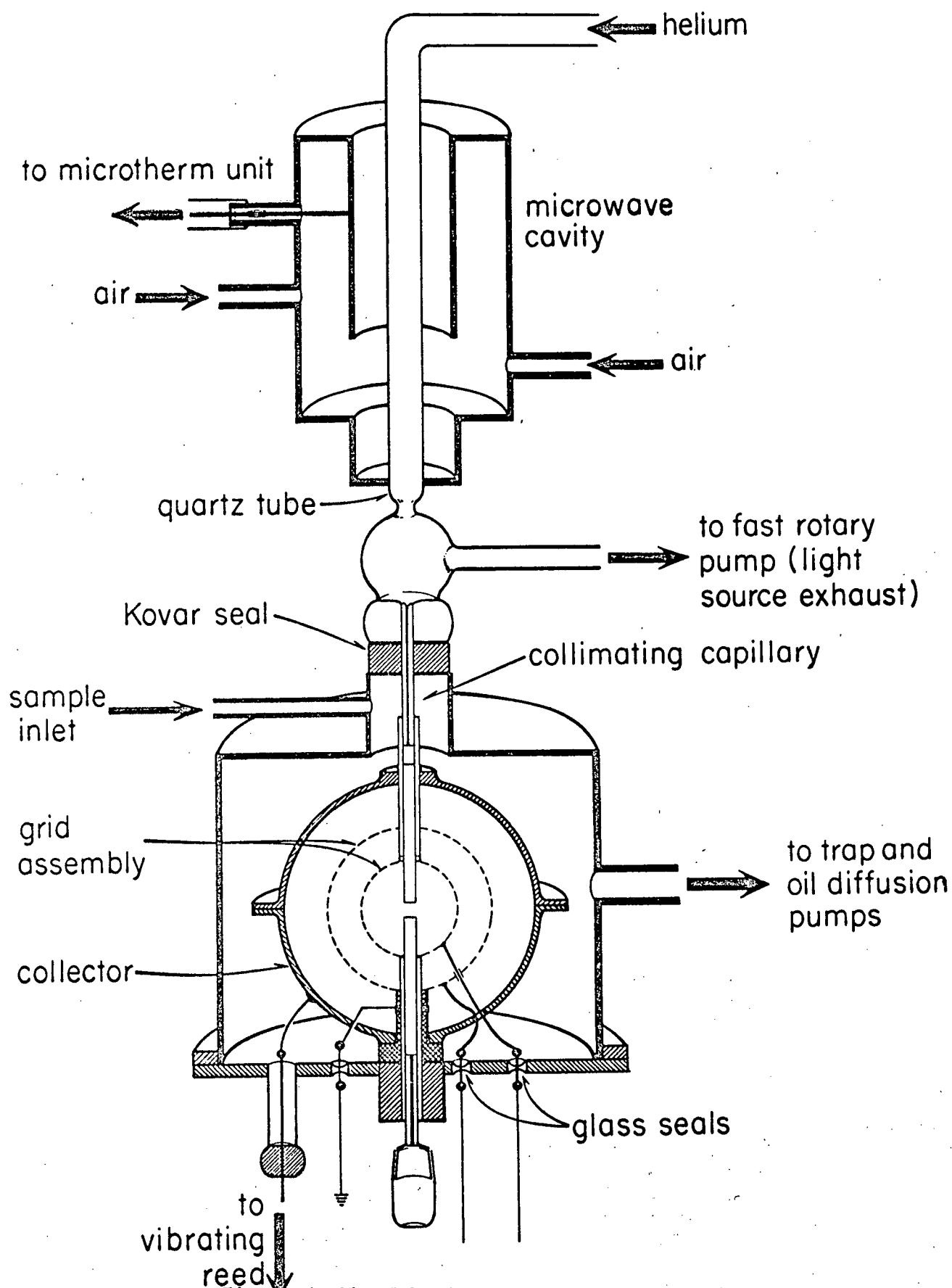


Figure 4 The Spherical Photoelectron Spectrometer

inch) were used. The new grids were more spherical and transparent, 56% against 45% with the etched brass. Both these factors helped in improving the resolution. Further improvement in resolution came with the use of only one spherical grid in the analyzer (41). The retarding field is then applied between the single erstwhile 'inner' grid and the collector. By this method all the positive ions (which were previously repelled by a positive potential between the two grids) now reach the collector. This presents no problem, however, since the positive current background remains constant. This arrangement decreases the electron scattering between the central ionization region and collector and improves the resolution by a factor of two. The photoelectron stopping curve for argon is used to illustrate the energy resolution attainable with one and two grids is shown in Figure 5. The former arrangement results in a peak half width of only 0.045 eV, compared with double this for the latter, and will obviously be advantageous in the detection of fine structure in photoelectron spectra.

In the work reported here two spherical grids were used, since the single grid modification only occurred very recently.

B.. The Samples used and their handling system.

The compounds used in this work and their origins are shown in Table I. Mass spectral analysis showed them to be free from any impurities which might cause ambiguities in the photoelectron stopping curves.

COLLECTOR CURRENT (I)

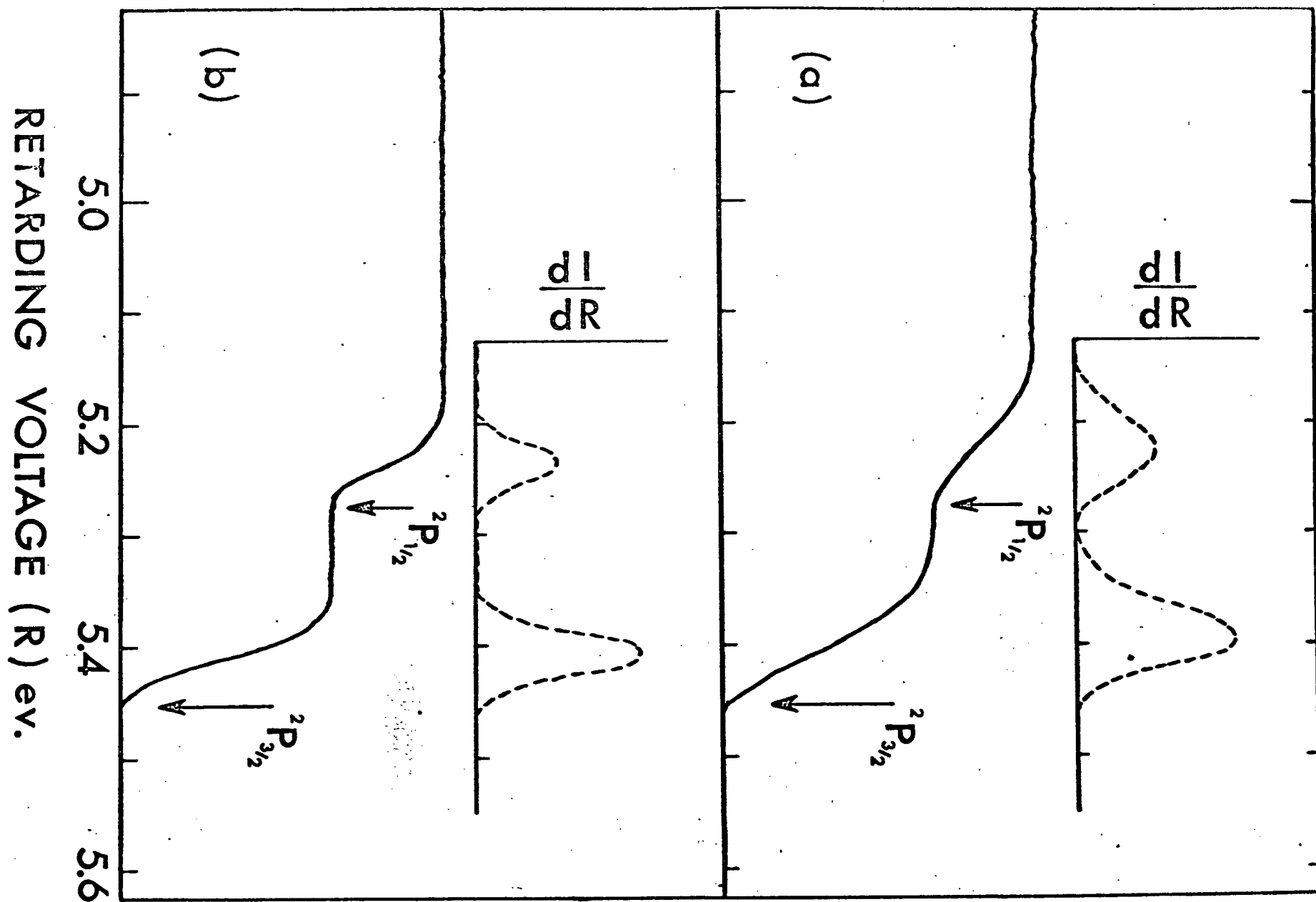


Figure 5. Photoelectron Spectrum of Argon obtained (a) with double, (b) with single grid in the energy analyzer.

Table I

Sample	Grade	Origin
Methyl Iodide	Spectroscopic	Baker and Adamson Products
Methyl Bromide	Reagent	British Drug House
Methyl Chloride		Matheson of Canada Ltd.
Methyl Cyanide	Spectroscopic	Eastman Kodak
Ethyl Cyanide	Reagent	Eastman organic chemicals
Acetaldehyde	Reagent	Eastman organic chemicals
Acetone	Spectroscopic	Eastman organic chemicals
Sulfur Hexafluoride		Matheson of Canada Ltd.

Sample Handling System

Figure 6 shows a diagram of the sample handling and vacuum system. Gases are introduced directly into the reservoir R (to a pressure of ~ 1 mm Hg) from the gas sample container. Taps T_1 and T_3 are initially open while taps T_2 , T_4 and T_5 are closed. After the sample is introduced into the reservoir, taps T_1 and T_3 are closed and T_5 opened, so that the vapour (after its initial expansion into R) enters the spectrometer through a 'metrosil' molecular leak

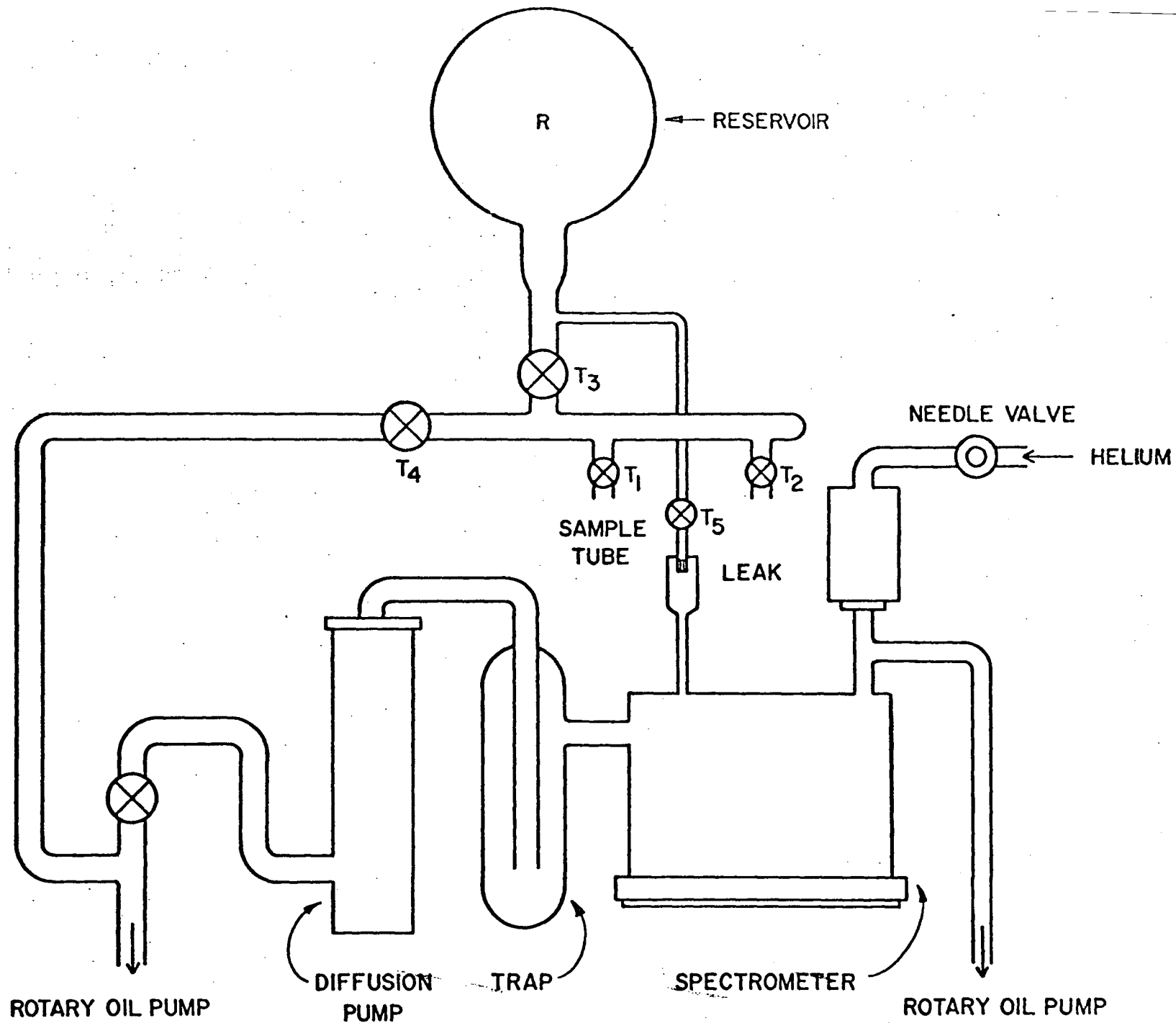


Figure 6. The Sample Handling and Vacuum System.

(sintered glass) at the required rate. The leak dimensions are such that about a millimeter reservoir pressure results in an ionization gauge pressure of 5×10^{-4} mm Hg. The ionization chamber pressure is probably an order of magnitude greater than this. For liquid samples the procedure followed was slightly different. They are first placed in the tube and degassed by repeated freezing in liquid nitrogen, pumping off and melting. Finally the vapour is introduced into the reservoir. The system is evacuated by a Welch duo-seal rotary oil pump and is controlled by tap T_4 . All the taps are greased with Apiezon M.

C. The Photoelectron Spectrometer

The essential components of the spectrometer, shown in Figure 4, are:

- 1) The Photon Source
- and 2) The Photo-electron Energy Analyzer.

1. The Photon Source

The photon source is the 584 \AA (21.21 eV) resonance emission from a microwave discharge in helium. Tank helium (Canadian Liquid Air Co) at a pressure of ~ 20 microns flows through the axial quartz discharge tube. Flow control is achieved with an Edwards high vacuum OSIC stainless steel needle valve. The discharge takes place in a resonant cavity, and the power is supplied by a Raytheon Microtherm 100 watt 2450 mc/s generator. The inside of the cavity is silver plated for high efficiency. Differential pumping and a 5 cm long 0.5 mm

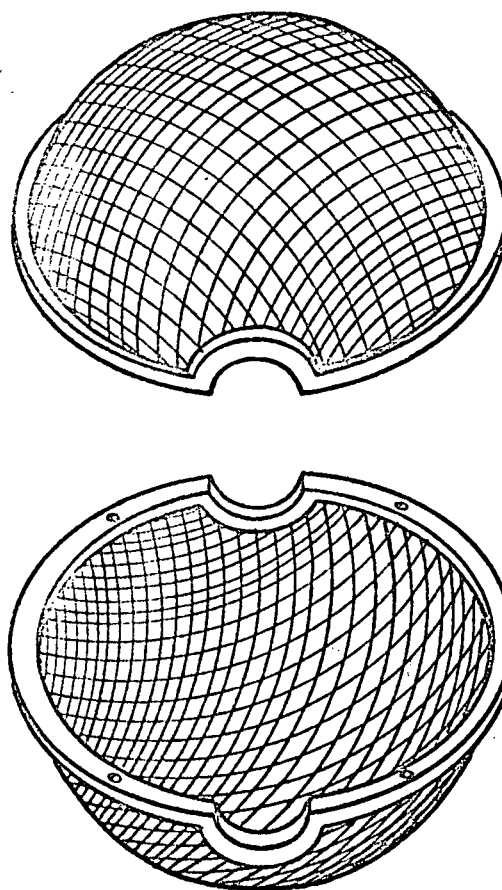


Figure 7. A Spherical Grid.

diameter collimating capillary effectively prevent the helium from entering the analyzer. The source is forced air cooled.

2. The Photoelectron Analyzer

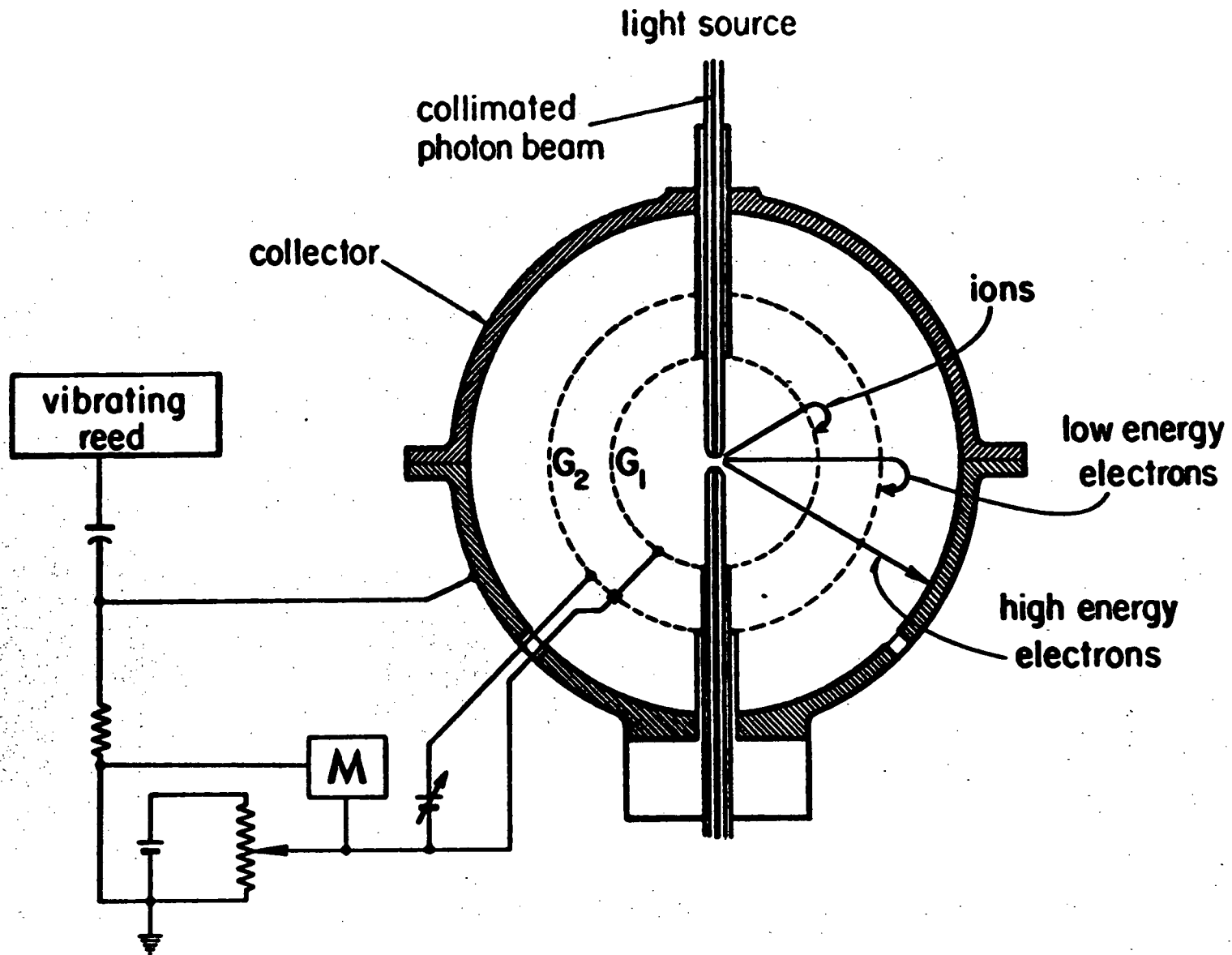
The analyzer consists of two concentric spherical grids and a collector. The grids (1.5 and 2 inches internal diameter) are pressed from 50 by 0.003 inch diameter stainless steel mesh, giving a theoretical transparency of 75% each. A diagram of the grids appears in Figure 7.

As shown in Figure 4, the inner grid is kept in position by two photon conducting tubes of gold plated brass. These two tubes are equipotential to the inner grid, and so the space enclosed by the inner grid and the two tubes is electric field-free.

The collector, internal diameter 3 inches, is turned from solid brass and is gold plated. The inner surface is coated with a colloidal suspension of graphite ("Aquadag"). The purpose of this is to minimize the reflection of photoelectrons. The whole analyzer is enclosed in a cylinder of "mumetal" to reduce internal magnetic fields and so maximize the resolution. All the spacers are made of pyrex, and electrical leakage between the outer grid and the collector is minimized by placing an earthed nickel disc between the two teflon spacers. The sample gas flows in through 1/4 inch diameter holes in the collector near the photon beam axis.

3. Operation of the Spectrometer

In the central field-free region the photon beam interacts with sample molecules to form ions and photo-electrons. A constant



SPHERICAL PHOTOELECTRON SPECTROMETER

Figure 8. Schematic Diagram of Electron Retarding System.

potential difference of 3 volts is maintained between the inner and outer grids - sufficient to prevent positive ions from passing through the outer grid into the electron retarding field. The photoelectron retarding voltage is applied between the inner grid and the collector from a ten turn 20,000 ohm double-ended helipot. The collector is grounded through the vibrating reed electrometer.

An electron ejected from a molecule in the field free region moves to the inner grid. It is then accelerated to the second grid and decelerated as it moves towards the collector. The photoelectron energy spectrum is scanned by decreasing the retarding potential difference between the inner grid and the collector at 1 volt per minute by a Heller 2 T 60 variable speed motor, connected through a friction clutch to the helipot spindle. This method of scanning the electron energy spectrum is similar to that used by Schoen (33), but differs from that used by Al-Joboury and Turner (31,32).

A Cary model 31 Vibrating Reed Electrometer amplifies the collector current, finally displayed on a Leeds and Northrup strip chart recorder. The photoelectron retarding voltage is read from a digital voltmeter, and a push button event control marker is used to produce spiked reference pulses every 0.1 volt on the chart. After the completion of every scan, the run is repeated with no sample gas present and the background so obtained subtracted from the original signal to obtain the true photoelectron spectrum.

4. Vacuum System

Since scattering of the electrons by neutrals could distort the retarding potential curves, it is desirable to work at as low a

pressure as possible. The main spectrometer is pumped by a C.E.C. 'MCF 60' oil diffusion pump fitted with a 'dry ice'-cooled cold-trap, and backed by a Welch duo-seal rotary oil pump. The same rotary oil pump is used to evacuate the sample reservoir. An ionization gauge mounted over the cold trap is used to measure sample pressure. The background pressure is usually about 1×10^{-5} mm Hg.

The light source differential pumping is provided by a similar Welch duo-seal rotary oil pump to that used for the main vacuum system.

CHAPTER III

The Methyl HalidesExperimental details

The sources and purities of the sample gases are given below. Krypton was used as a calibrating gas and the ionization

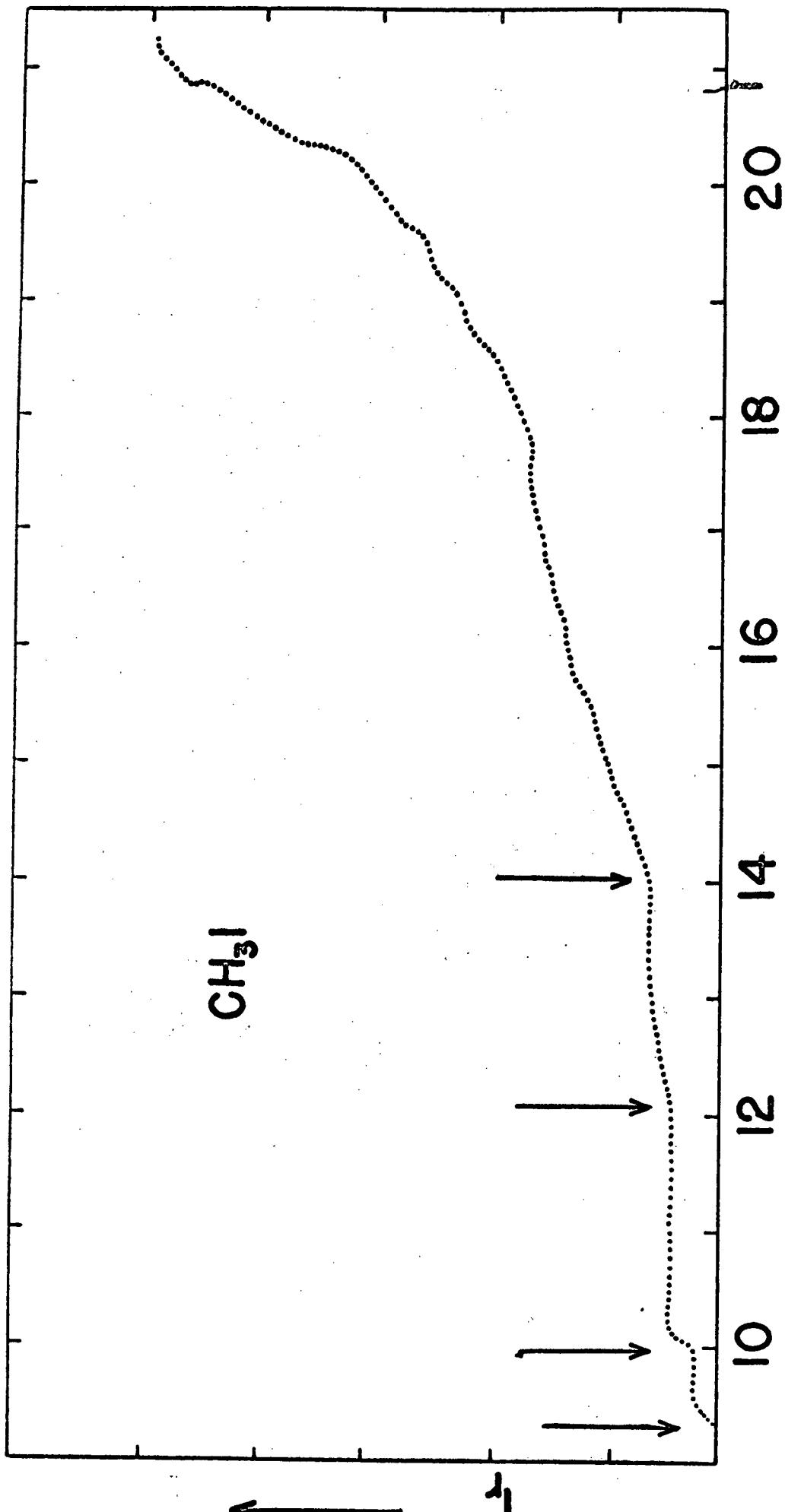
Table II

Sample	Grade	Origin
Methyl Iodide	Spectroscopic	Baker and Adamson products
Methyl Bromide	Reagent	British Drug House
Methyl Chloride		Matheson of Canada Ltd.

potentials were determined with it and the unknown compound both in the photoelectron spectrometer at the same time. Prior to each set of experiments the resolution of the instrument was tested by its ability to resolve the argon doublet (of 0.18 eV separation). The gas pressures used in this work were of the order of 5×10^{-4} mm. of mercury for CH_3I , CH_3Br and CH_3Cl .

Experimental Results

The photoelectron current versus ionizing energy curves



(21.21-R)eV

Figure 9. Photoelectron Spectrum of Methyl Iodide.

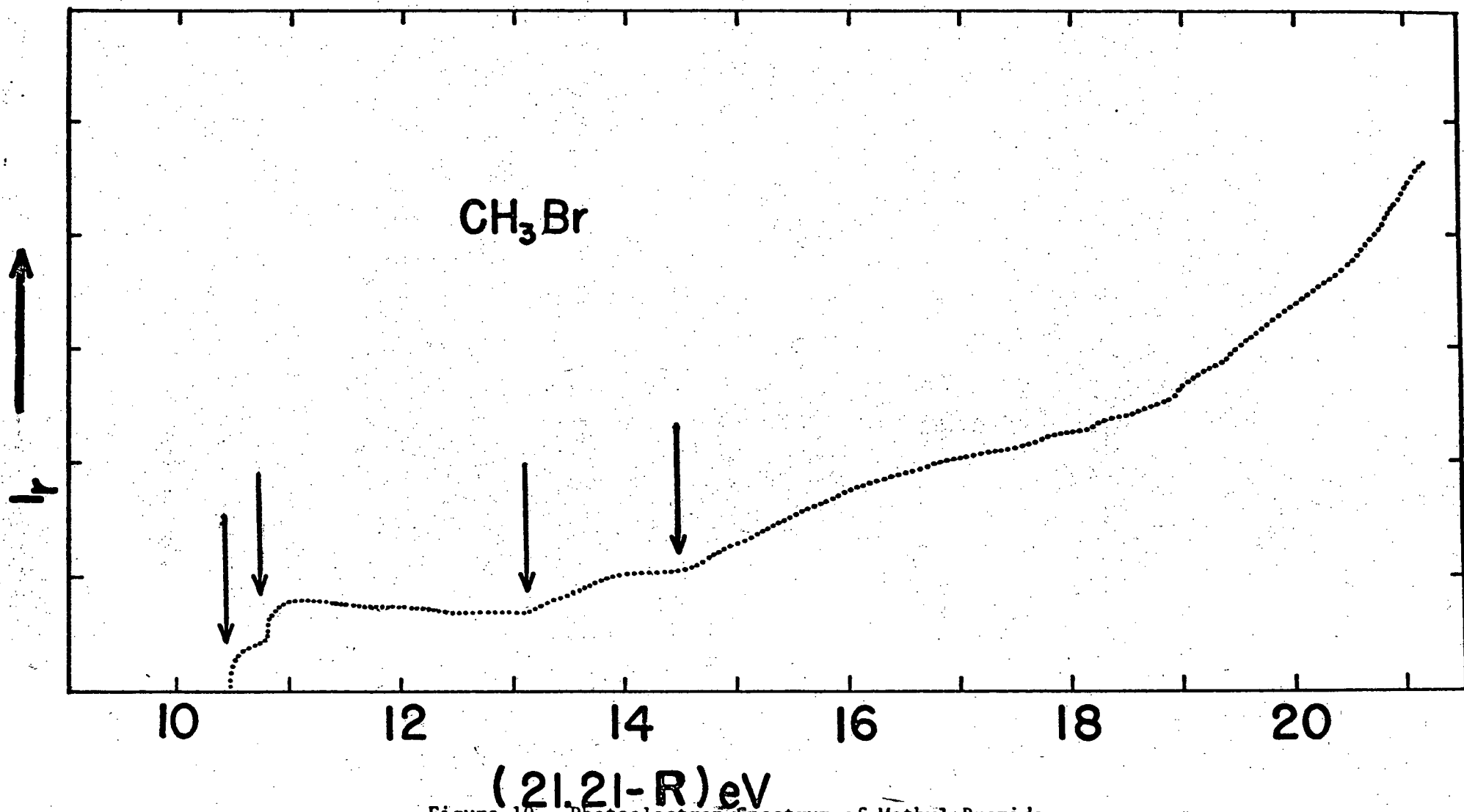


Figure 10. Photoelectron Spectrum of Methyl Bromide.

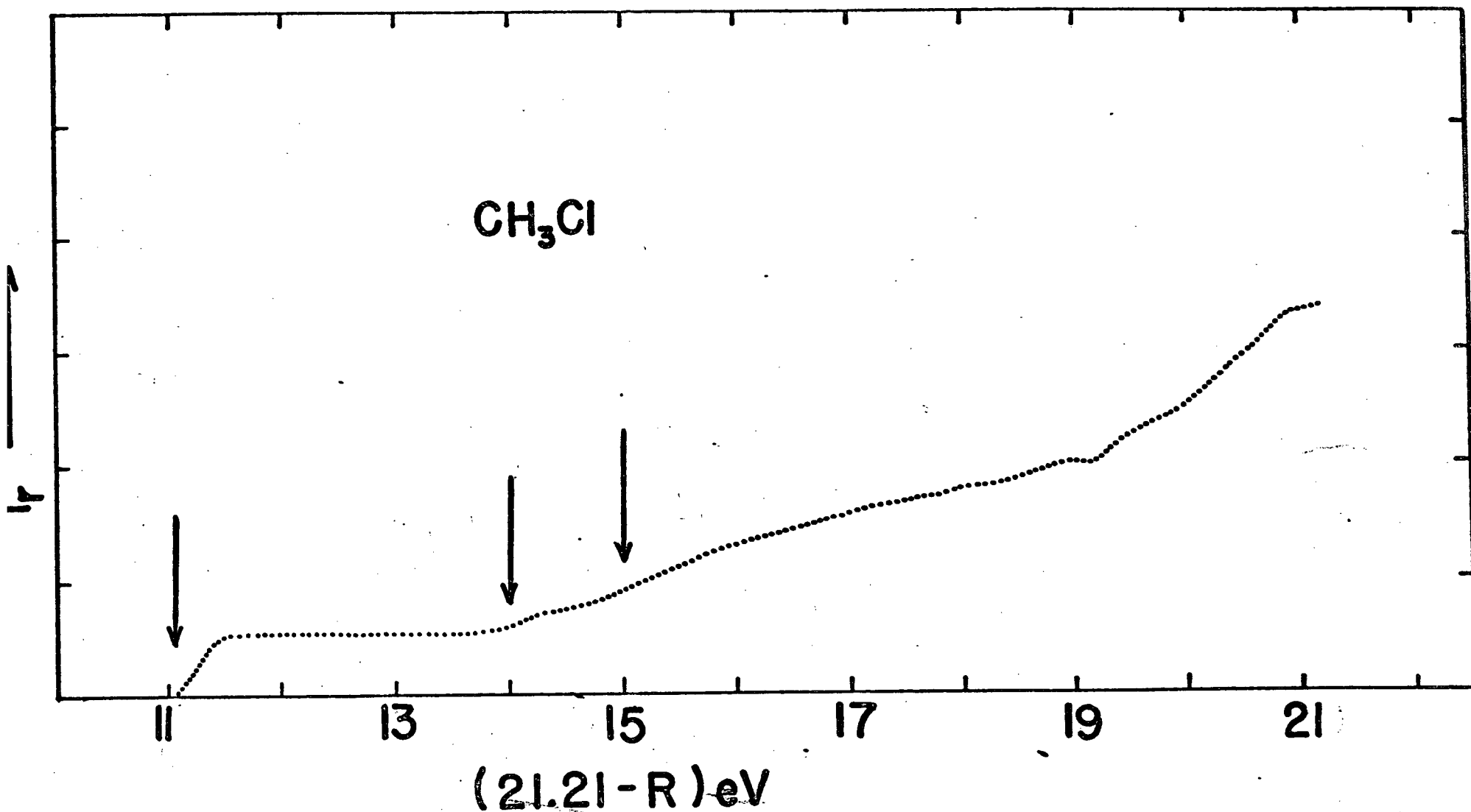


Figure 11. Photoelectron Spectrum of Methyl Chloride.

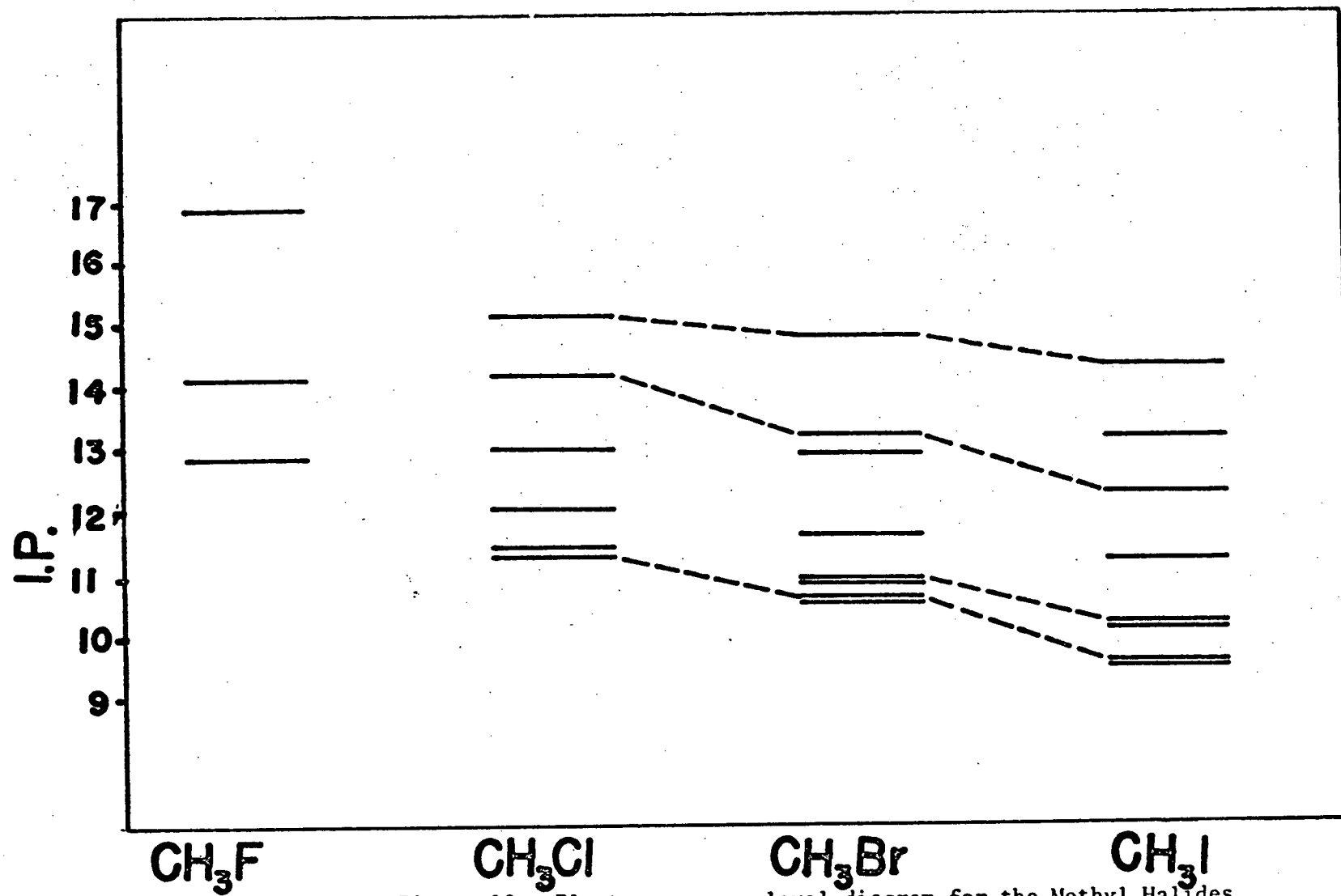


Figure 12. Electron energy level diagram for the Methyl Halides.

corrected for background are plotted in Figures 9, 10 and 11 respectively. Figure 12 shows the orbital energy levels for the three methyl halides found here and in the electron impact studies of Frost and McDowell (42) using monoenergetic electrons. The photoelectron stopping curves for methyl iodide and methyl bromide shown in Figures 9 and 10 clearly indicate the formation of these ion species in four different states. These are deduced to be the $^2E_{1/2}$, $^2E_{3/2}$, 2A_1 and 2E state. This is in agreement with the electron impact studies done by Frost and McDowell (42) Tsuda, Melton and Hamill (43) and the spectroscopic studies of Price (44). The corresponding components of the CH_3Cl^+ ground states are not resolved however. Frost and McDowell (42) were also unable to resolve this doublet, but Tsuda, Melton and Hamill (43) report its separation in their electron impact studies. For this ion only three different processes have been detected, and they lead to CH_3Cl^+ in the ground 2E and excited 2A and 2E electronic states. Reasons for the assignment of the ionization processes are given in the discussion, and the various electron impact, spectroscopic and photoionization ionization potentials of the methyl halides found by different workers are summarized in Table III.

Discussion

The methyl halides all have a similar nuclear arrangement and belong to the pyramidal symmetry C_{3v} . Their electronic structure may be represented (47) by the formula:

$$(1s_c)^2 [Sa_1]^2 (nS_{x a_1})^2 (\pi e)^4 [\sigma a_1]^2 (np\pi_{x e})^4, {}^1A_1 \quad (3-1)$$

Table III
Ionization potentials of the Methyl Halides (eV)

Compound	Spectroscopic (44)	Photoionization		Electron Impact		This Work
		Watanabe (45)	Nicholson (46)	Frost & McDowell (42)	Tsuda & Hamill (43)	
<u>Methyl Iodide</u>						
(1st I.P.)	9.49 (² E _{1/2})	9.54	9.55	9.51 (² E _{1/2})	9.50	9.56 ± 0.01 (² E _{1/2})
(2nd I.P.)	10.11 (² E _{3/2})		10.12	10.09 (² E _{3/2})	10.00	10.19 ± 0.02 (² E _{3/2})
(3rd I.P.)				11.22 (² A ₁)	11.20	12.29 ± 0.02 (² A ₁)
(4th I.P.)				13.14 (² E _{3/2, 1/2})	13.10	14.30 ± 0.01

Table III (Continued)

Compound	Spectroscopic	Photoionization		Electron Impact		This Work
		Watanabe	Nicholson	Frost & McDowell	Tsuda & Hamill	
	(44)	(45)	(46)	(42)	(43)	
<u>Methyl Bromide</u>						
(1st I.P.)	10.49	10.53	10.52	10.53	10.50	10.55 \pm 0.01
	(² E _{1/2})			(² E _{1/2})		(² E _{1/2})
(2nd I.P.)	10.80		10.86	10.85	10.80	10.86 \pm 0.02
	(² E _{3/2})			(² E _{3/2})		(² E _{3/2})
(3rd I.P.)				11.62	11.50	13.22 \pm 0.03
				(² A ₁)		(² A ₁)
(4th I.P.)				12.94	12.90	14.79 \pm 0.05
				(² E _{3/2} , 1/2)		

Table III (Continued)

Compound	Spectroscopic	Photoionization		Electron Impact		This Work
		Watanabe	Nicholson	Frost & McDowell	Tsuda & Hamill	
	(44)	(45)	(46)	(42)	(43)	
<u>Methyl Chloride</u>						
(1st I.P.)	11.17	11.28	11.26	11.42	11.30	11.29 \pm 0.02
	($^2E_{1/2}$)			($^2E_{1/2}$)		($^2E_{1/2}$)
(2nd I.P.)	11.25		11.34		11.40	
	($^2E_{3/2}$)					
(3rd I.P.)				12.07	11.90	14.14 \pm 0.04
				(2A_1)		(2A_1)
(4th I.P.)				13.02	13.20	15.14 \pm 0.05
				($^2E_{3/2, 1/2}$)		

where $n = 3, 4$, or 5 for CH_3Cl , CH_3Br and CH_3I respectively. The inner electrons are omitted and the orbitals are written in order of decreasing binding energy.

Mulliken (47) has discussed the molecular orbital formulae of these compounds and has shown that their structures can be understood better if they are compared with that of methane. The structure of CH_4 (symmetry T_d) is (48).

$$(1S_c)^2 (Sa_1)^2 (pt_2)^6, {}^1A_1 \quad (3-2)$$

If we suppose one H atom slightly displaced the symmetry can be reduced to C_{3v} . As a consequence of this operation there are certain alterations in the molecular orbitals.

From group theory it is known that the completely symmetrical representations of all symmetry groups correlate. The methane $[Sa_1]^2$ orbital is completely symmetrical but the $[pt_2]^6$ is not, and so it is essential to determine how the latter orbital correlates with the representations of the methyl halide symmetry group C_{3v} . It is also known from group theory (47, 49) that the triply degenerate T_2 correlates with the A_1 and E representations of the group C_{3v} , so when the CH_4 symmetry is reduced from T_d to C_{3v} the triply degenerate $[pt_2]$ orbitals will split up into a symmetric $[\sigma a_1]$ and a doubly degenerate pair $[\pi e]$ and lead to an expression similar to that given in (3-1) for the methyl halides:

$$[1S_c]^2 [Sa_1]^2 [\pi e]^4 [\sigma a_1]^2, {}^1A_1 \quad - (3-3)$$

The twofoldly degenerate $[\pi e]$ here should have nearly the

same energy as the $[\pi e]$ in the methyl halides. Each is confined essentially to the CH_3 radical, and the only differences are due to secondary effects in shape and field of force within the CH_3 which result when a C-I is substituted for a C-H bond.

In equation (3-2), the () brackets refer to mainly atomic non-bonding orbitals and the square brackets refer to molecular orbitals, although $[\pi e]$ is completely, and $[\text{Sa}_1]$ largely localized on the CH_3 radical. The orbital $[\sigma]$ is the main C-H bonding orbital.

The first ionization potential corresponds to the removal of an electron from the $(n\pi_{\text{Xe}})$ orbital, non-bonding and largely localized on the halogen atom. Some evidence for this comes from the shape of the photoelectron stopping curves for the methyl halides in Figures 9, 10 and 11 respectively, where a sharp step for the first process is seen indicative of the removal of a non-bonding electron. This would leave the molecular ion in a ^2E electronic state, having two components, $^2\text{E}_{1/2}$ and $^2\text{E}_{3/2}$, due to spin-orbital interaction.

When the molecular ion CH_3X^+ is formed it is to be expected that the singly occupied orbital will be to a large degree localized around the halide atom. If this is the case then the separation of the ionic ground state spin-orbital components for each methyl halide would be expected to approximately equal the separation pertaining in the corresponding halogen atom and hydrogen halides. Furthermore, since for atoms the doublet energy separation resulting from spin-orbital interaction is proportional to the fourth power of the atomic number (50), it follows that the $^2\text{E}_{3/2} - ^2\text{E}_{1/2}$ ground state separations for the CH_3X^+ ions should increase with the atomic weight

of the halogen atom from the chloride to the iodide. The experimental results in Table IV bear out this expectation (51). It is clear from Figures 9 and 10 that for CH_3I^+ and CH_3Br^+ the doublets due to spin-orbital interaction have been resolved. That this interpretation is correct is shown by far ultraviolet studies of these molecules by Price (44), photoionization studies by Nicholson (46), and electron impact studies by Frost and McDowell (42) and Tsuda, Melton and Hamill (43). In 1936, Price found two Rydberg series in this spectral region for methyl iodide and their limits were 0.62 eV apart. Mulliken (47) interpreted these limits as corresponding to the two spin-orbital components of the ^2E ionic ground state. The value of 0.63 eV found in this work agrees well with the spectroscopic value. The values 0.58 eV and 0.50 eV found by Frost and McDowell (42) and Tsuda, Melton and Hamill (43) by electron impact studies are slightly lower.

In the case of methyl bromide, Price (44) found two Rydberg series having a separation of 0.31 eV between their limits. Frost and McDowell (42) found this separation to be 0.32 eV, and Tsuda, Melton and Hamill (43) found a value of 0.30 eV. In this work the $^2\text{E}_{1/2} - ^2\text{E}_{3/2}$ separation is found to be 0.31 eV, again in good agreement with the previous studies. For CH_3Cl^+ , the ^2E ground state doublet separation would be expected to be less than 0.1 eV. From Figure 11, it is clear that we have been unable to resolve these components. However Price (44) found two Rydberg series having a separation of 0.08 eV between their limits.

Table IV

Spin-orbital Interaction energies of Methyl Halide Ions (eV)

Ion	Worker	Method	Doublet Separation
CH_3I^+	This work	Photoelectron spectroscopy	0.61
	Price (44)	Spectroscopic	0.62
	Frost & McDowell (42)	Electron impact	0.59
	Tsuda, Melton & Hamill (43)	Electron impact	0.50
	Nicholson (46)	Photoionization	0.57
	Morrison (52)	Photoionization	0.60
CH_3Br^+	This Work	Photoelectron spectroscopy	0.31
	Price (44)	Spectroscopic	0.31
	Frost and McDowell (42)	Electron impact	0.32
	Tsuda, Melton & Hamill (43)	Electron impact	0.30
	Nicholson (46)	Photoionization	0.33

The next inner ionization potential above those associated with the methyl halide doublet ground state should refer, according to equation (3-1) to the removal of an electron from the C-X orbital $[\sigma_{\text{a}1}]$. This would lead to the formation of CH_3X^+ ions in their $^2\text{A}_1$ excited electronic states. Through a comparison of data of this work for

three methyl halides it is possible to say that the process just described is correct. The value found in this work for the removal of an electron from the CH_3I $[\sigma a_1]$ orbital is 12.29 eV, for CH_3Br and CH_3Cl being 13.22 and 14.14 eV respectively.

The next ionization potential above that involving the $[\sigma a_1]$ orbital should, from equation (3-1), refer to the removal of an electron from the doubly degenerate $[\pi e]^4$ bonding orbital localized in the methyl group. The $[\pi e]^4$ orbital, being derived from the $[\pi t_2]$ orbital of methane when the symmetry is altered from Td to C_{3v} , should have an I.P. approximately equal to the first I.P. of methane, 13.16 eV. The values observed for this ionization process in this work are 14.30 eV for methyl iodide, 14.79 eV for methyl bromide, and 15.14 eV for methyl chloride. The increase in value could be easily accounted for by CH_3 being more positively charged due to the presence of the electro-negative atoms chlorine, bromine and iodine in the methyl halides.

Acetaldehyde

Acetaldehyde, acetone and formaldehyde are the simplest set of compounds containing the group $>C=O$. It is well known that the double bond in these compounds is associated with high polarity and hence it is to be expected that the molecules' ionization potentials will be strongly influenced by charge transfer. Previous results are available for the first ionization potentials of these molecules and will be referred to below. The work to be described here shows how the binding energies of some of the more strongly bound orbitals differ from the values obtained by Sugden and Price (53), who studied these molecules using a monoenergetic (photo) electron impact technique. They found a number of breaks in the ionization efficiency curves which they assumed to be inner I.P.'s

Experimental details

The acetaldehyde was an Eastman Kodak sample and was of reagent grade purity, and a pressure of 5×10^{-4} mm of mercury was maintained in the system. The acetone used was spectroscopically pure and the calibration gas was krypton in both cases.

Experimental Results

The photo-electron stopping curve for acetaldehyde is shown in Figure 13. The curve shows clearly that there are four distinct processes leading to ionization and these occur at 10.22 ± 0.01 , 12.89 ± 0.1 , $13.98 \pm .04$ and 15.10 ± 0.02 eV.

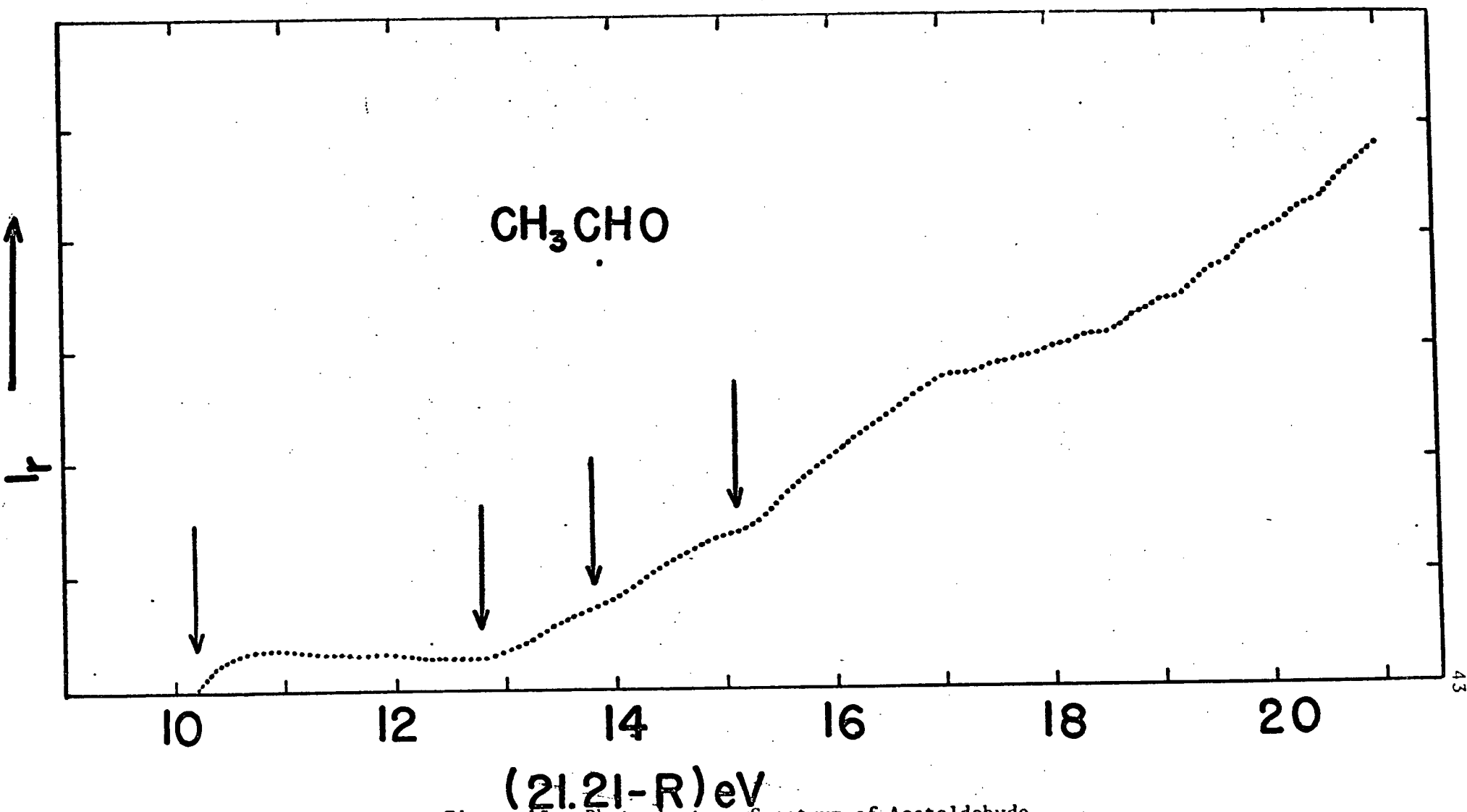


Figure 13. Photoelectron Spectrum of Acetaldehyde.

Discussion

Mulliken (54) has described the electronic structure of acetaldehyde as follows (1s electrons are omitted)

$$\begin{array}{ccccccccccc} (2S)^2 & [S]^2 & [S]^2 & [x+x]^2 & [y]^2 & [Z+Z]^2 & [\Pi]^4 & (2 p_y)^2 & , & ^1A \\ 0 & CH_3 & HCC-O & CO & HCC & HCC-O & CH_3 & O & & \end{array} \quad (3-4)$$

The electronic structure is essentially that of formaldehyde with the CH_3 orbitals $[S]^2 [\Pi]^4$ added, and in $[y]$, $[Z+Z]$, and the second $[S]$, the C of CO is bonded to one H and one C instead of to two H's as in H_2CO . No representation symbols have been used in equation (3-4), the symmetry of H_2CO (C_{2v}) having been largely destroyed. Strictly speaking there is interaction and mixing amongst all the various orbitals given in equation (3-4).

From equation (3-4) the first ionization potential of acetaldehyde would be expected to refer to the removal of a $(2 p_y)$ electron from the O atom. Walsh (55) found three Rydberg series all leading to the same limit at 10.18 eV, and he deduced that a non-bonding, electron was being removed since the series members were remarkably free from vibrational structure. Mulliken (54) has also shown that the lowest ionization potential in these simple aldehydes corresponds to the removal of a non-bonding $2 p_y$ electron from the oxygen atom. The first ionization potential observed in this work at 10.22 eV therefore should correspond to ionization of the $2 p_y$ non-bonding orbital. The shape of the stopping curve confirms the non-bonding character of the orbital. The first ionization potential found in this work agrees well with photoionization values of 10.21 eV by Watanabe (45), and of 10.25 eV by Hurzeler, Inghram and Morrison (56)

The value of 10.4 eV found by Sugden and Price (53) using the electron impact technique seems to be rather high.

The first four ionization potentials found in this work are given in Table V. Also included are the results of Sugden and Price (53).

Table V
Ionization Potentials of Acetaldehyde (eV)

This Work	Electron impact Sugden and Price (53)
10.22 \pm 0.01	10.40
12.89 \pm 0.01	11.30
13.98 \pm 0.04	12.30
15.10 \pm 0.02	13.50

It is evident from Table V that the agreement between the first ionization potential obtained by the two methods is good, but for higher energy processes the values differ widely. The electron impact results, however could be complicated by interference from pre-ionization.

We assign the value at 12.89 to ionization from the C-C bond, bearing in mind the possible hybridisation between the γ and S bonding electrons in this respect. The ionization potential of C_2H_6 is 11.8 eV, and this corresponds to the removal of an electron from

the C-C bonding (σa_1) orbital. The higher value in our case could be due to the presence of the strongly electro-negative oxygen atom.

In equation (3-4) the $[Z+Z]$ and $[x_o + x_c]$ electrons provide the σ and π bonding of the carbonyl group. The predicted ionization potential for $[x_o + x_c]$ from valence state data on the basis of the simple equation (54) $I > \frac{1}{2} [\bar{I} (2p_o) + \bar{I} (2p_c)]$,

$$\text{with } \bar{I} = 17.17 \text{ eV for } 2p \text{ oxygen atom} \quad (57)$$

$$\bar{I} = 11.21 \text{ eV for } 2p \text{ of carbon atom} \quad (57)$$

is slightly greater than 14.2 eV. The charge transfer is largely due to these electrons, and consequently a reduction in the ionization potential is predicted. These qualitative arguments show that the value at 13.89 eV is by no means unreasonable for the ionization potential of the $[x_o + x_c]$ orbital.

As pointed out by Mulliken (54) the ionization potential for $[\pi]$ of CH_3 is predicted to be approximately the same as for $[\pi]$ of CH_3 in CH_4 or CH_3I , for which the estimated value is 14.4 eV. The fourth ionization potential found in this work at 15.1 eV, therefore, may well correspond to removal of an electron from $[\pi]$ of the CH_3 bonding orbital. This value is somewhat larger than that estimated by Mulliken probably because the CH_3 group here is more positively charged owing to the presence of the strongly electro-negative oxygen atom. Interaction with $(2 p_y)$ O should also tend to increase the ionization potential of $[\pi]$, the ionization potential of $(2p_y)$ O being decreased at the same time.

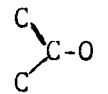
Acetone

The experimental results obtained for acetone are shown in Figure 14. In the case of acetone there are seen to be four different ionization processes leading to ionization. They correspond to ionization potentials of 9.72 ± 0.01 , 12.11 ± 0.02 , 13.8 ± 0.04 and 15.40 ± 0.01 eV, and as expected, they fall generally into line with the results for acetaldehyde.

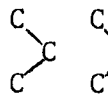
For acetone a configuration similar to equation (3-4) can be written, but with an [S] and [Π] group for each CH_3 . The molecular orbital formula (54) is:

$$[2S]^2[S]^2[S]^2[S]^2 [x + x]^2[y]^2[z + z]^2[\Pi]^4[\Pi]^4(2p_y)^2; {}^1A,$$

O
 CH_3

CH_3


$\text{C}-\text{O}$
 $\text{C}-\text{O}$



CH_3

CH_3
 O

(3-5)

The lowest I.P. (9.72 eV) obviously corresponds to the non-bonding electron $2p_y$, and has been observed as the culmination of a Rydberg series by Duncan (58) at 10.20 eV, appreciably higher than the value found in the present work. Watanabe's (45) photoionization value for this process is $9.69 \pm .01$ eV in excellent agreement with the present value. The electron impact method gives the first ionization potential of acetone as 9.92 eV (Morrison and Nicholson (59)), 10.2 eV (Sugden and Price (53)), and 10.1 eV (Noyes (60)). Recently Al-Joboury and Turner (61) found the first ionization potential of acetone to be 9.67 eV by photoelectron spectroscopy. It is noted that the electron impact figures are considerably higher than the value found in this work, and this is probably due to the relatively low ionization cross-section at threshold.

The ionization potentials obtained in this work together with the results of Al-Joboury and Turner, and Sugden and Price are given in Table 6.

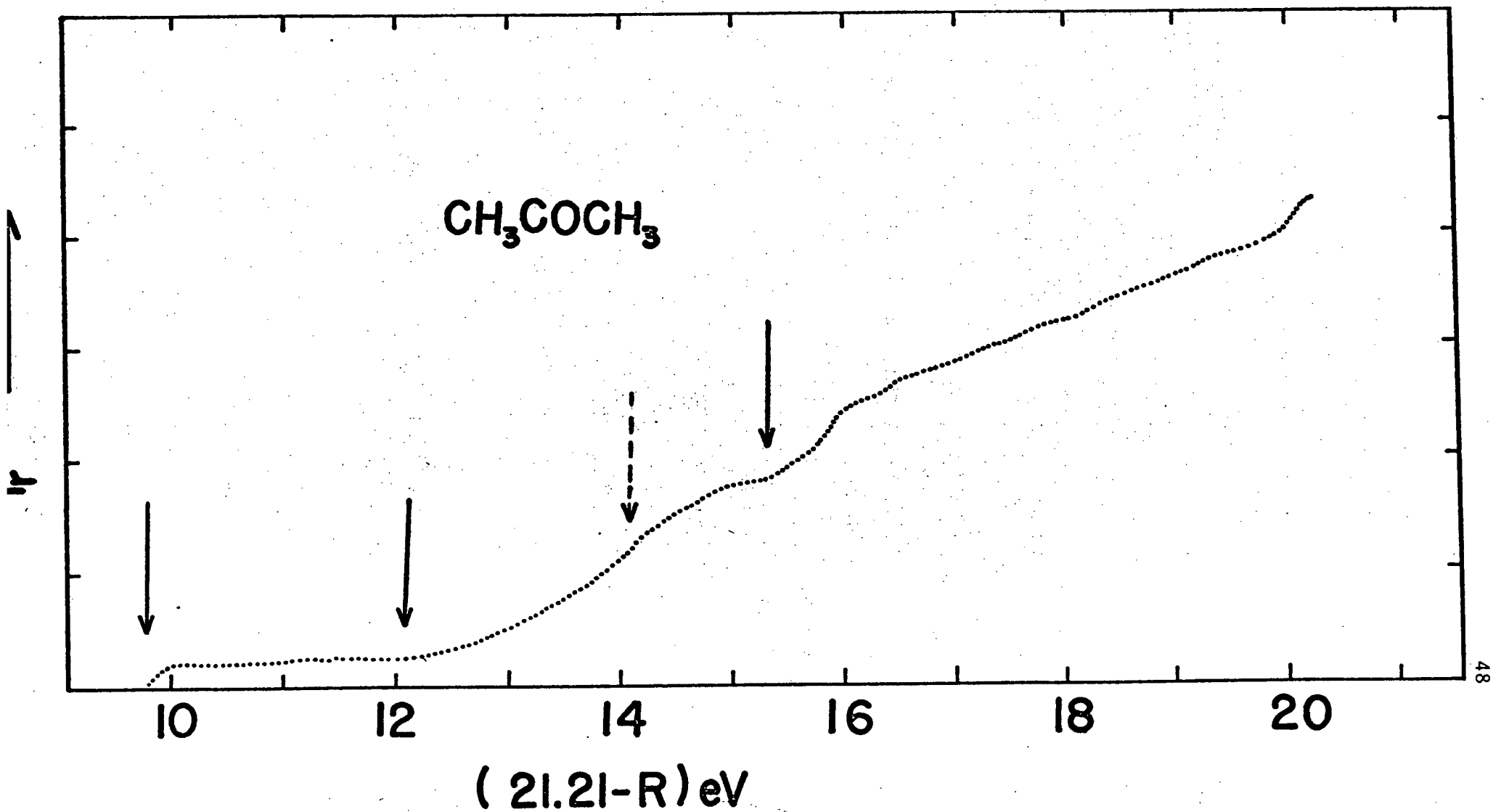


Figure 14. Photoelectron Spectrum of Acetone.

Table 6

Ionization potentials of Acetone (eV)

This Work	Al-Joboury and Turner (61)	Sugden and Price (53)
9.72 \pm 0.01	9.67	10.2
12.11 \pm 0.02	12.16	11.3
13.80 \pm 0.04	14.15	12.2
15.40 \pm 0.01	15.55	13.6

No spectroscopic data is available on the inner ionization potentials of acetone however it is clear from the Table 6 that evidence for the four ionization processes seen in the photo-electron spectrum obtained by Al-Joboury and Turner (61) is in good agreement with the present work. Such is not the case with the values obtained by Sugden and Price (53) for three inner ionization potentials.

Sulfur Hexafluoride

The sulfur hexafluoride molecule is known to have the form of a regular octahedron from the results of electron diffraction measurements and from studies of the Raman and infrared spectra (62). No photoelectron spectrum of this molecule has been reported previously. The far-ultraviolet absorption spectrum has been studied by Moe and Duncan (64) and Codling (65). Using the electron-impact method,

Dibeler and Mohler (66), Marriot and Craggs (67) and Fox and Curran (68) have indicated that the most probable ionization product is the SF_5^+ ion and that its ionization threshold is about 15.8 eV. Very recently, Dibeler and Walker (69) measured the photoionization efficiency between 1050 and 600 Å by means of a combined vacuum-UV monochromator and mass spectrometer while Simpson, Kuyatt and Miliczarek (70) measured the absorption spectrum of SF_6 in the far ultraviolet by electron impact.

Experimental

The sample of SF_6 was obtained from Matheson of Canada Ltd. and was of high purity. Argon was used as a calibrating gas.

Experimental Results

The photoelectron spectrum from SF_6 , determined at an incident photon energy of 584 Å, is shown in its integrated form in Figure 15. Electron current is plotted against (21.21 eV minus R, the retarding voltage) so that the binding energy can be read directly off the abscissa. There are four ionization thresholds clearly in evidence, and these occur at 15.35, 16.71, 18.11 and 19.5 eV.

Discussion

The first two thresholds observed at 15.35 eV and 16.71 eV during this work correspond with SF_5^+ photoionization thresholds obtained by Dibeler and Walker (69), and the third with what appears to be a definite increase in their photoionization efficiency at about 18.2 eV. The process occurring at 19.50 eV could either be due to SF_4^+ formation or to another SF_5^+ threshold, - there appears to be a slight increase

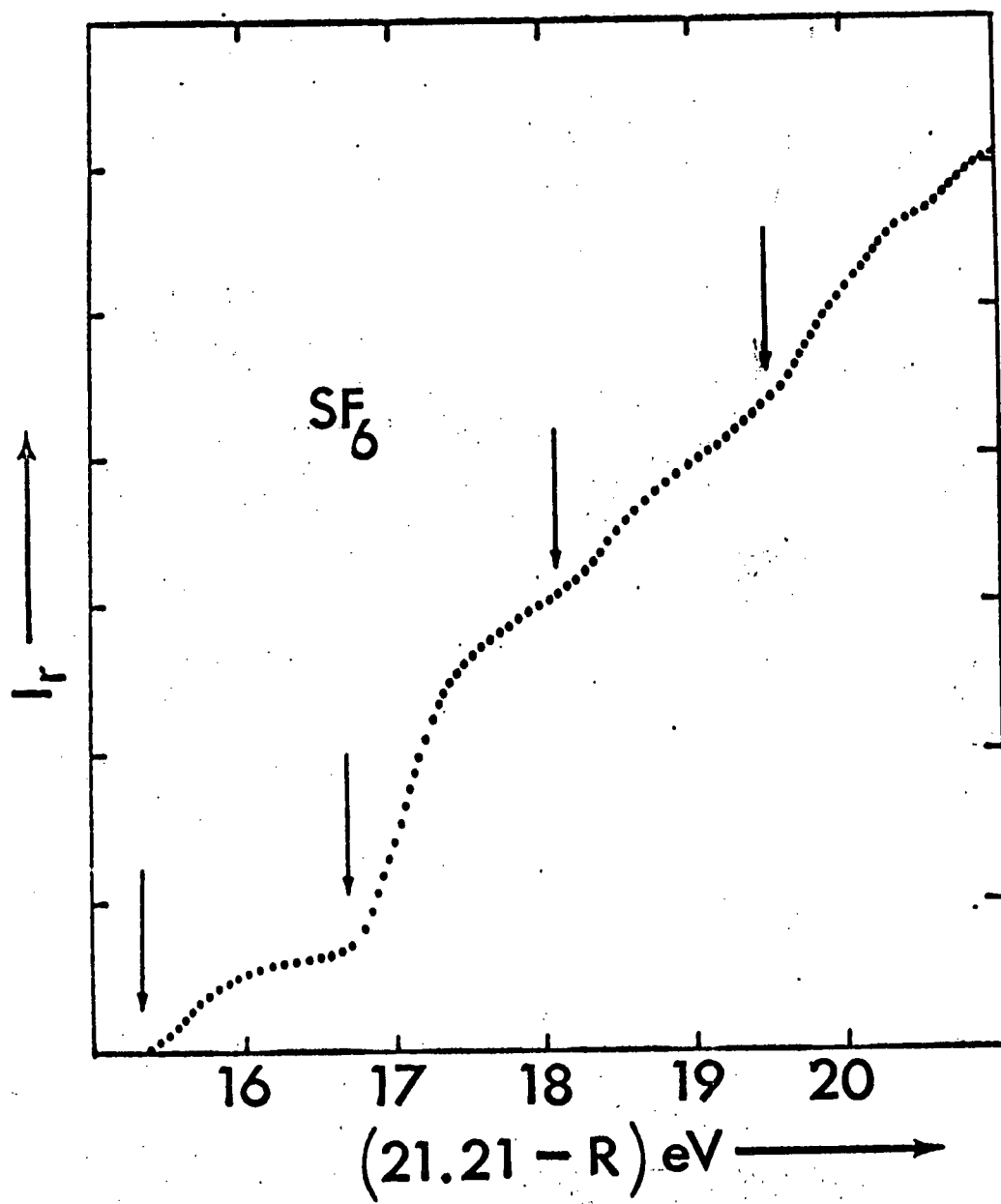


Figure 15. Photoelectron Spectrum of Sulfur-Hexafluoride.

in Dibeler's curve at this energy. Fox and Curran (68) have reported electron impact (RPD) SF_5^+ thresholds at 15.85, 17.0 and 18.0 eV. Although the first is 0.56 eV higher than the SF_5^+ photoionization threshold, the other two correlate reasonably well with our 16.7 and 18.1 values.

Although no mass analysis is employed in this work the ions produced below 19 eV can be taken to be almost exclusively SF_5^+ since the relative abundance of SF_6^+ is only 3×10^{-4} that of SF_5^+ and other positive ions have appearance potentials above 19 eV. Direct comparison of our photoelectron spectrum may therefore be made with the SF_5^+ fragment photoionization curve from SF_6 .

The relative (maximum) intensities of the 15.29 and 16.53 eV processes as measured by Dibeler and Walker are about 1:2, whereas ours are about 1:3. The difference is either due to the effects of preionization unresolved in the direct ionization experiment or to a greater fall-off in the cross-section for the first process at a photon energy of 21.21 eV.

It is interesting to note that the U-V absorption cross-section of SF_6 derived from inelastic electron scattering measurements (70) shows two maxima of almost equal intensity at energies corresponding to our first two thresholds. That our relative intensities are so much more in agreement with Dibeler and Walker's supports their suggestion that electron impact non-ionizing processes may be responsible for the discrepancy.

Methyl and Ethyl Cyanides

No work concerned with the inner ionization potentials of

these molecules has been reported in the literature, even though methyl halides have been studied by many workers. It was the purpose of this work to determine the inner ionization potentials of these molecules and to attempt to correlate them with the electronic structures as given by McDowell (71).

Experimental

The methyl cyanide was a spectroscopically pure sample. The ethyl cyanide was supplied by Eastman organic chemicals and was found to be free from detectable impurities (mass spectral analysis). Krypton was again used as a calibrating gas.

Experimental Results

The photoelectron stopping curves for CH_3CN^+ are shown in Figures 16 and 17 respectively. The energies at which the steps are observed in the curves are given in Table 7 below. Figure 18 gives the orbital energy level diagram for HCN, CH_3CN and $\text{C}_2\text{H}_5\text{CN}$. The values for HCN are taken from electron impact studies (72) using the R.P.D. technique.

Discussion

Infra-red studies (73) have shown that the methyl cyanide molecule has symmetry C_{3v} like the methyl halides. Its electronic structure can be derived by the same method employed for the methyl halides, i.e. it is regarded as a derivative of a methane which has been distorted so that it has a symmetry C_{3v} . McDowell (71) has described the electronic structure of methyl cyanide as follows:

$$\begin{aligned} &----[S_n+S_c, \sigma a_1]^2 [S_n-S_c, \sigma a_1]^2 [Sa_1]^2 [\sigma_c+\sigma_c, a_1]^2 \\ &\quad \quad \quad [\pi_n+\pi_c, e]^4 [\pi e]^4 \end{aligned} \quad (3-6)$$

Table 7

Ionization potential of methyl cyanide and ethyl cyanide (eV)

Compound	Ionization Potentials (eV)
Methyl Cyanide	12.23 \pm 0.01
	12.52 \pm 0.01
	13.17 \pm 0.04
	15.29 \pm 0.10
Ethyl Cyanide	11.8 \pm 0.02
	12.83 \pm 0.02
	13.47 \pm 0.02
	16.29 \pm 0.03

(The inner orbitals are omitted)

In this formulation the $[\pi e]$ orbitals are assumed to be largely localized in the methyl group. $[\sigma_c + \sigma_c, a_1]^2$ is the main c - c bonding orbital, the $[\pi_n + \pi_c, e]^4$ represents the two degenerate π bonding orbitals of the CN group which are mutually perpendicular.

The spectroscopic value of 11.96 eV reported by Cutler (74) for the first ionization potential of methyl cyanide is based on a poorly characterized Rydberg series of only three members. Miss Cutler mentions several experimental difficulties encountered in her work. The first ionization potential observed in this work at 12.23 eV is in good agreement with the photoionization data of 12.22 \pm 0.01 eV by Watanabe (25), 12.205 \pm 0.004 eV by Nicholson (46) and 12.33 eV by Mak (75). Previous determinations of the electron impact first

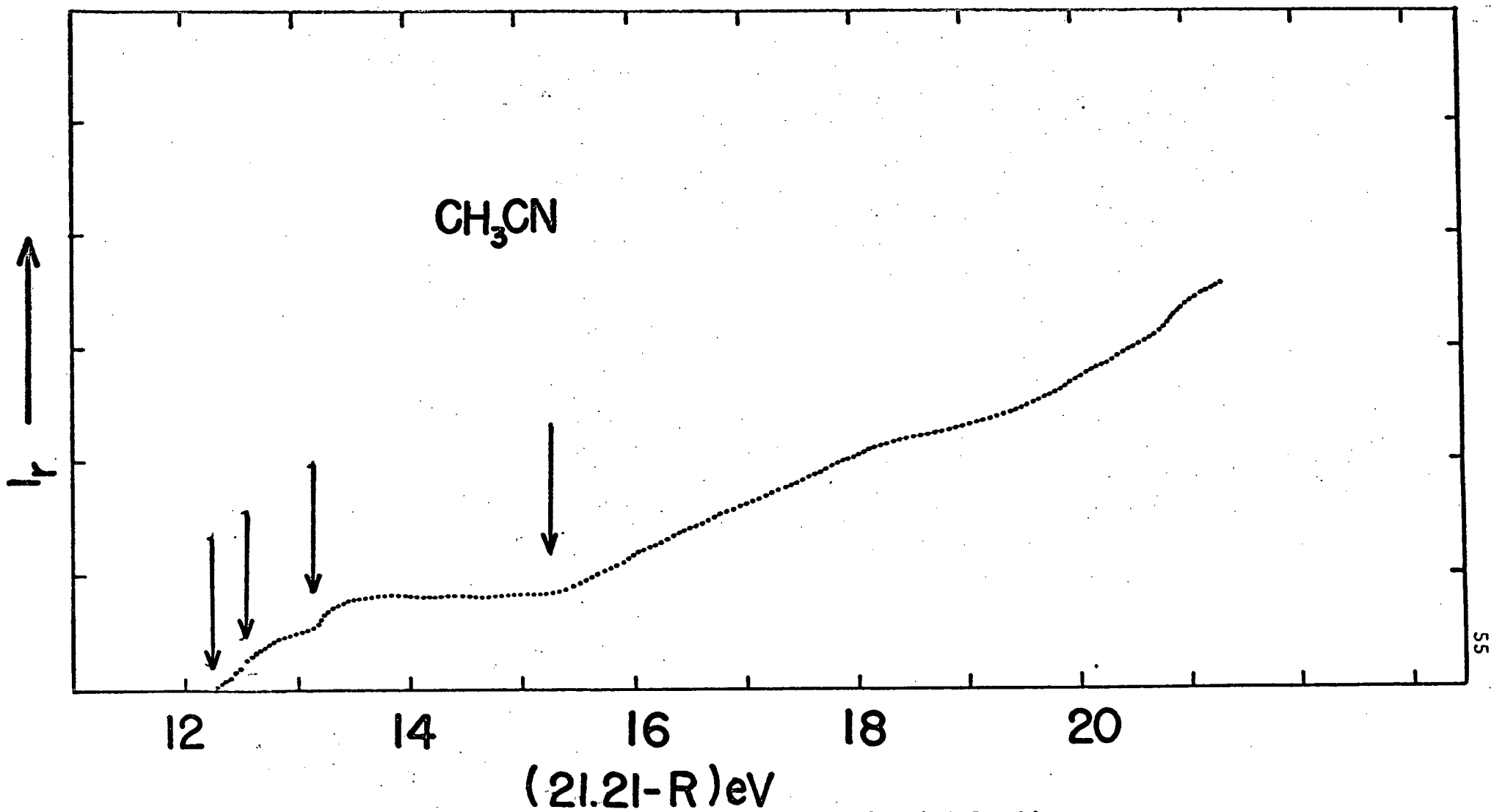


Figure 16. Photoelectron Spectrum of Methyl Cyanide.

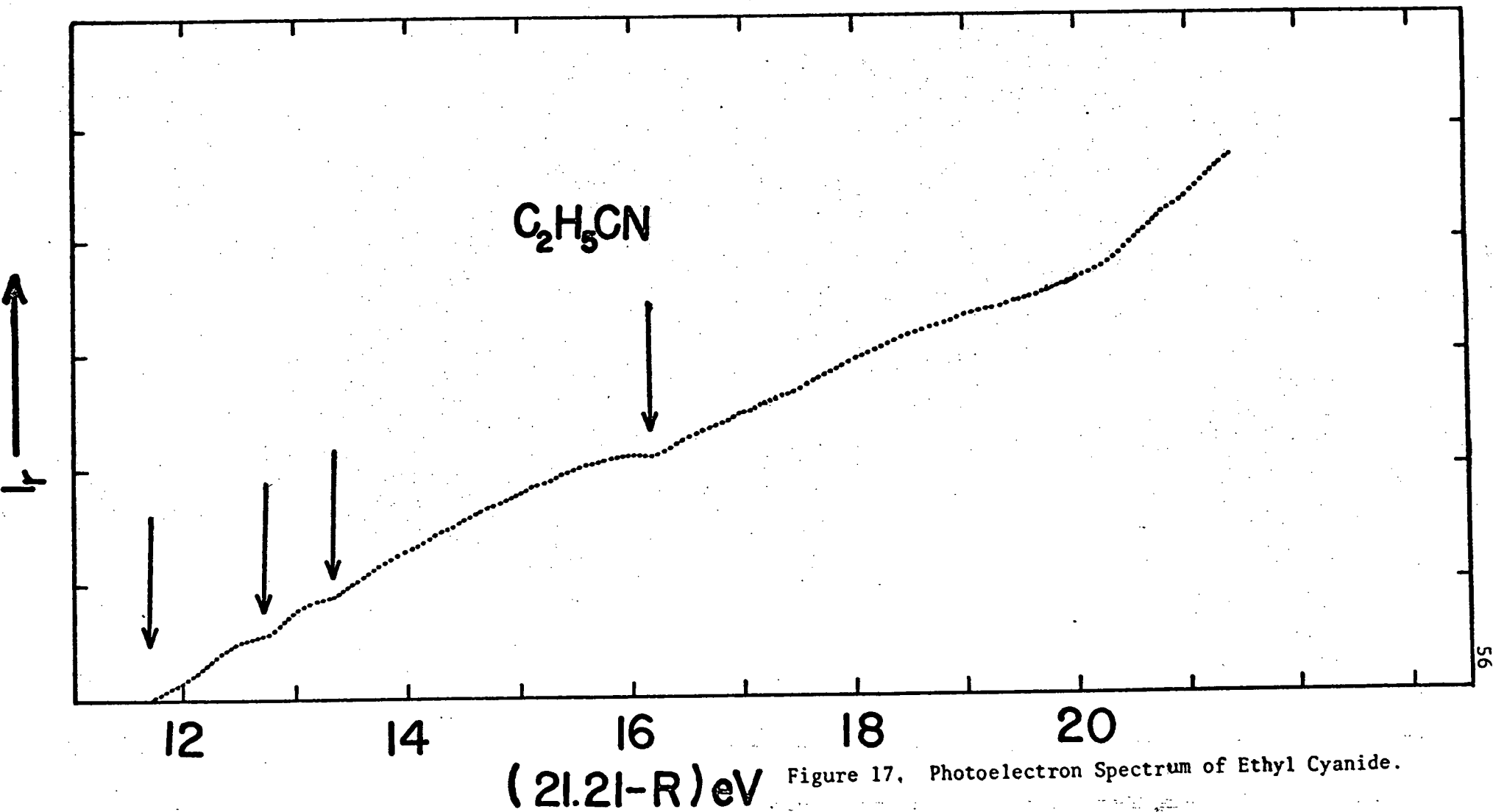


Figure 17. Photoelectron Spectrum of Ethyl Cyanide.

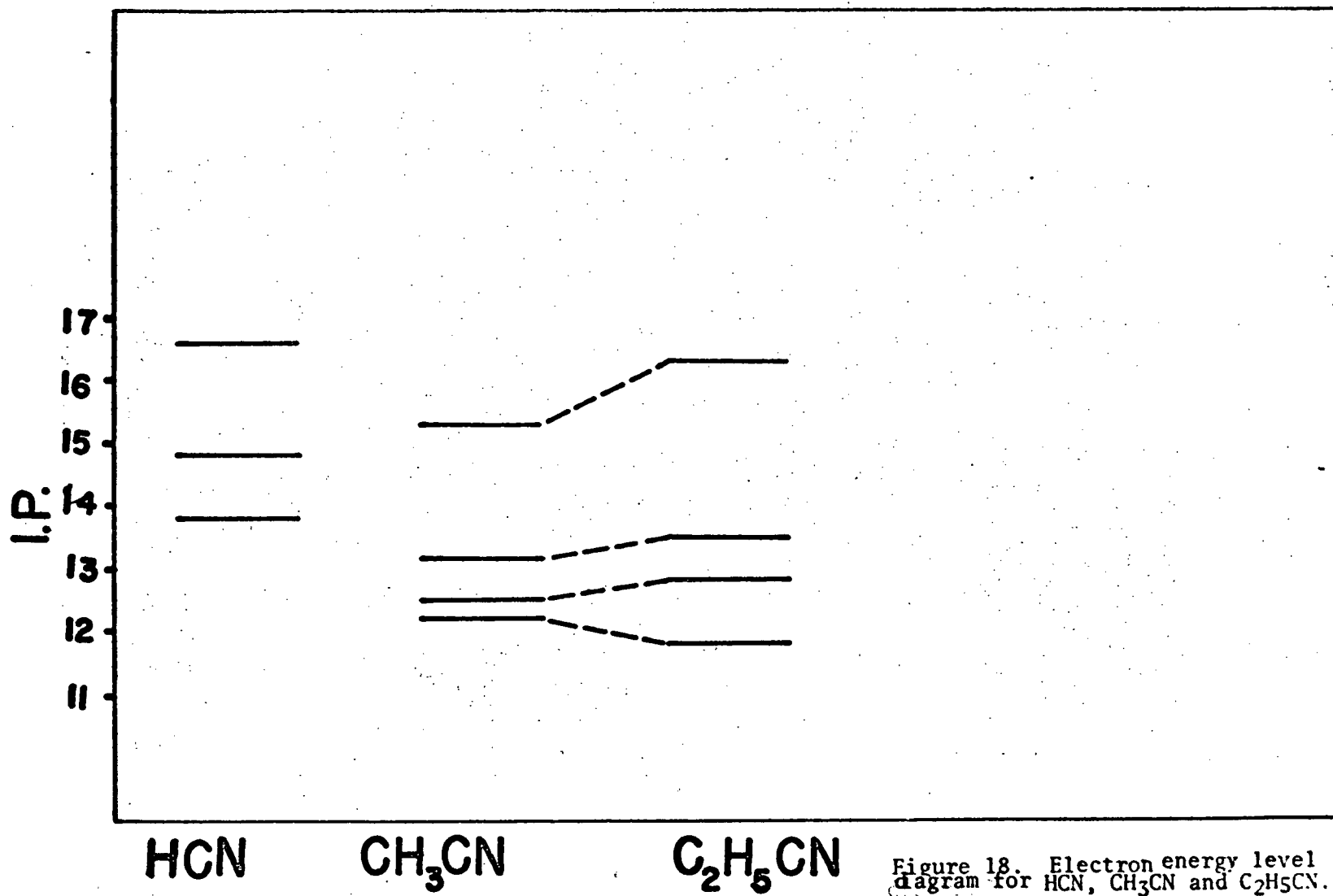


Figure 18. Electron energy level diagram for HCN, CH₃CN and C₂H₅CN.

ionization potential have been made by McDowell and Warren (12.52 eV) (59).

The first ionization potential of methyl cyanide refers to the removal of a $[\sigma_C + \sigma_C, a_1]$ bonding electron, the bonding character being determined from the shape of the photoelectron stopping curve for this process. The identification of this process is assured for the following reasons. The dissociation energy of the C-C bond in ethane is 3.68 eV and $D(\text{CH}_3\text{-CN})$ is known to be 5.8 eV (77). Relative dissociation energies can be taken as a reasonable measure of the relative firmness with which electrons are bound in the bonding orbitals. It is, therefore, to be expected that the ionization potential of an electron in the $[\sigma_C + \sigma_C, a_1]$ orbital of CH_3CN would be higher than that for an electron in the $[\sigma a_1]$ orbital of ethane, i.e. greater than 11.8 eV. Further support comes from the fact that a methyl group when attached to a resonating system behaves as if it were conjugated to the attached group (78, 79). The contribution of these conjugated structures can be easily seen from the C-C bond distance in the molecule. The C-C bond distance in this case is 1.459 Å (80) which corresponds to about 17 percent double bond character and hence to a 17 percent contribution of these conjugated structures. Thus the first ionization potential of CH_3CN could well lie at 12.23 eV.

As pointed out by McDowell (71) there will be some interaction between the π orbitals of the methyl and CN groups. This will lead to two new molecular orbitals of the type $(\pi_{\text{CH}_3} + \pi_{\text{CN}})$ and $(\pi_{\text{CH}_3} - \pi_{\text{CN}})$, and so two new energy levels will arise. It is therefore

suggested that the second ionization potential found here at 12.5 eV refers to the removal of an electron from the $(\pi_{\text{CH}_3} + \pi_{\text{CN}})$ orbital, and that the third ionization potential at 13.17 eV arises from ionization of the $(\pi_{\text{CH}_3} - \pi_{\text{CN}})$ orbital.

The fourth ionization potential at 15.29 eV is presumed to refer to the removal of an electron from the $[S_N + S_C, \sigma a_1]$ bonding orbital. Spratley (72) found a value of 16.59 eV in case of HCN for occurrence of this process. The increase in value in the latter case can be attributed to highly electropositive nature of the hydrogen atom.

Ethyl Cyanide

Ionization potentials are observed for $\text{C}_2\text{H}_5\text{CN}$ at 11.8 eV, 12.83 eV, 13.47 eV and 16.29 eV.

The value found for the first ionization potential at 11.8 eV is in fair agreement with the electron impact figure of 11.85 eV found by Morrison and Nicholson (59) and the photoionization value of 11.84 eV found by Watanabe (25). This process will refer to the removal of an electron from the C-C bond.

In the case of $\text{C}_2\text{H}_5\text{CN}$ the first ionization potential is lower, while the second and third ionization potentials are higher than the corresponding ones in CH_3CN . The differences be understood on the basis of hyperconjugation. In case of CH_3CN we expect the C-C bond to be somewhat strengthened by becoming an acceptor bond drawing its new strength from the "donor" bonds on either side (79). This is not true in the case of $\text{C}_2\text{H}_5\text{CN}$, however since as pointed out by

Coulson (78) the degree of hyperconjugation is a maximum in the case of a CH_3 group and to a lesser extent for a CH_2CH_3 and other alkyl radicals. One would therefore expect the C-C bond to be weaker and the two Π bonds to be stronger in the case of $\text{C}_2\text{H}_5\text{CN}$.

It seems from this information that the value of 11.8 eV associated with the ionization from the C-C bond would not be unreasonable. The values of 12.83 eV and 13.47 eV are assigned to the two Π orbitals (these orbitals arise from the interaction of Π orbitals of methyl group with Π orbitals of the CN group). The fourth I.P. at 16.29 is presumed to refer to the removal of an electron from the N-C σ bonding orbital.

CONCLUSION

In the present work, it has been shown that the photoelectron spectroscopic technique can be used to determine I.P.'s of molecules to an accuracy of 0.01 eV. The method is capable of indicating the existence of excited electronic states of molecular ions, and in favourable cases it is also possible to determine the bonding or anti-bonding nature of the ionized orbital from the shape of the photoelectron stopping curve. In addition, the ordinary photon and electron impact techniques fail to distinguish between ionization limits and auto-ionization in the strong resonance transitions of inner electrons. The photoelectron method is not directly affected by autoionization, and the inner I.P.'s are not obscured by these autoionization peaks.

In this work the photoelectron spectra from eight molecules have been determined at an incident photon energy of 584 \AA (21.21 eV). A suitable extension of this work would be the use of mono-chromatic radiation of higher energy in order to enable the removal of inner shell electrons. Experiments both of this type and involving the measurement of angular dependence of photoelectron ejection are in progress in this laboratory.

In this study it has been shown that a Single Grid Photoelectron Spectrometer will be advantageous in the detection of fine structure in photoelectron spectra, although it may prove to be difficult to measure the relative transition probabilities to the various vibronic states owing to the constant positive-ion background.

REFERENCES

1. F. H. Field, J. L. Franklin, "Electron Impact Phenomena", Academic Press, New York, (1957).
2. G. G. Hall, J. Lennard-Jones, Proc. Roy. Soc. A202, 155, (1950).
3. T. Koopmans, O. Physica, I, 104, (1933).
4. R. S. Mulliken, J. Am. Chem. Soc. 77, 887, (1955).
5. C. C. J. Roothaan, Rev. Mod. Phys. 23, 69, (1951).
6. G. W. King, "Spectroscopy and Molecular Structure", Holt, New York, (1964).
7. R. S. Mulliken, Phys. Rev. 46, 549, (1934).
8. R. S. Mulliken, J. Chem. Phys. 3, 514, (1935).
9. A. D. Walsh, Trans. Far. Soc. 42, 779, (1946).
10. G. G. Hall, J. Lennard-Jones, Proc. Roy. Soc. A205, 541, (1951).
11. C. E. Moore, Natl. Bur. Std. (U.S.) Circ. 467, (1958).
12. A. J. C. Nicholson, J. Chem. Phys. 29, 1312, (1958).
13. E.W. McDaniel "Collision phenomenon in ionized gases." John Wiley and Sons, Inc., New York, (1964).
14. E. M. Clarke, Can. J. Phys. 32, 764, (1954).
15. P. Marmet and L. Kerwin, Can. J. Phys. 38, 787, (1960).
16. R. E. Fox, W. M. Hickam, T. Kjeldaas, Jr., D. J. Grove, Phys. Rev. 84, 859, (1951).
17. C. E. Brion, D. C. Frost, C. A. McDowell, J. Chem. Phys. 44, 1034, (1966).
18. W. M. Hickam, R. E. Fox, T. Kjeldaas, Jr., Phys. Rev. 96, 63 (1954).
19. D. C. Frost, C. A. McDowell, Proc. Roy. Soc. A230, 227, (1955).
20. D. C. Frost, C. A. McDowell, Proc. Roy. Soc. A241, 194, (1957).

21. D. C. Frost, C. A. McDowell, Can. J. Chem. 36, 39, (1958).
22. R. E. Fox, W. M. Hickam, J. Chem. Phys. 22, 2059, (1954).
23. K. Watanabe, J. Chem. Phys. 22, 1564, (1954).
24. W. C. Walker, G. L. Weissler, J. Chem. Phys. 23, 1540, (1955).
25. K. Watanabe, T. Nakayama, J. Mutte, J. Quant. Spectrosc. Radiat. Transfer, 2, 369, (1962).
26. C. A. McDowell, "Mass Spectrometry" McGraw-Hill Book Company, Inc., New York, (1963).
27. F. P. Lossing and I. Tanaka, J. Chem. Phys. 25, 1031, (1956).
28. H. Hurzeler, M. G. Inghram, J. D. Morrison, J. Chem. Phys. 28, 76, (1958).
29. D. C. Frost, D. Mak, C. A. McDowell, Can. J. Chem. 40, 1064, (1962).
30. B. L. Kurbatov, F. I. Vilesov, A. N. Terenin, Doklady Akad Nauk. SSSR. 140, 797, (1961).
31. D. W. Turner, M. I. Al-Joboury, J. Chem. Phys. 37, 3007, (1962).
32. D. W. Turner, M. I. Al-Joboury, J. Chem. Soc. 5141, (1963).
33. R. I. Schoen, J. Chem. Phys. 40, 1830, (1964).
34. J. Franck, Trans. Far. Soc. 21, 536, (1925).
35. E. U. Condon, Phys. Rev. 28, 1182, (1926).
36. G. Herzberg, "Spectra of Diatomic Molecules", Second edition, Van Nostrand, New York, (1950).
37. R. W. Nicholls and A. L. Stewart, "Allowed Transitions in Atomic and Molecular Processes", Academic Press, New York, (1962).
38. R. W. Nicholls, J. Research Natl. Bureau Standards, 65A, 451, (1961).

39. D. C. Frost, C. A. McDowell, D. A. Vroom, Proc. Roy. Soc. A, (1967).
40. W. Heitler, "Quantum Theory of Radiation", third edition, Oxford, (1954).
41. D. C. Frost, J. S. Sandhu and D. A. Vroom, Nature. 212, 604, (1966).
42. D. C. Frost, C. A. McDowell, Proc. Roy. Soc. A241, (1957).
43. S. Tsuda, C. E. Melton, W. H. Hamill, J. Chem. Phys. 41, 689, (1964).
44. W. C. Price, J. Chem. Phys. 4, 539, (1936).
45. K. Watanabe, J. Chem. Phys. 26, 542, (1957).
46. A. J. C. Nicholson, J. Chem. Phys. 43, 1171, (1965).
47. R. S. Mulliken, Phys. Rev. 47, 413, (1935).
48. R. S. Mulliken, J. Chem. Phys. I, 492, (1933).
49. C. A. McDowell, Trans. Fara. Soc. 50, 423, (1954).
50. E. U. Condon, G. W. Shortley, "Theory of Atomic Spectra", Camb. Univ. Press, (1935).
51. C. A. McDowell and D. C. Frost, J. Chem. Phys. 24, 173, (1956).
52. J. D. Morrison, H. Hurzeler, M. G. Inghram, J. Chem. Phys. 33, 821, (1960).
53. T. M. Sugden, W. C. Price, Trans. Fara. Soc. 44, 116, (1948).
54. R. S. Mulliken, J. Chem. Phys. 3, 564, (1935).
55. A. D. Walsh, Proc. Roy. Soc. A185, 176, (1946).
56. H. Hurzeler, M. G. Inghram, J. D. Morrison, J. Chem. Phys. 28, 76, (1958).
57. R. S. Mulliken, J. Chem. Phys. 2, 782, (1934).
58. A. B. F. Duncan, J. Chem. Phys. 3, 131, (1935).

59. J. D. Morrison, A. J. C. Nicholson, J. Chem. Phys. 20, 1021, (1952).
60. W. A. Noyes, J. Chem. Phys. 3, 430, (1935).
61. M. I. Al-Joboury, D. W. Turner, J. Chem. Soc. 4434, (1964).
62. G. Herzberg, "Infrared and Raman Spectra of Polyatomic Molecules" Van Nostrand Company, Inc., New York, (1945).
63. T. K. Liu, G. Moe, A. B. F. Duncan, J. Chem. Phys. 19, 71, (1951).
64. E. D. Nostrand, A. B. F. Duncan, J. Am. Chem. Soc. 76, 3377, (1954).
65. K. Codling, J. Chem. Phys. 44, 4401, (1966).
66. V. H. Dibeler, F. L. Mohler, J. Res. Natl. Bur. Std. 40, 25, (1948).
67. J. W. Marriot, J. D. Craggs, Elec. Res. Assoc. Rept. L/T 300, (1953).
68. R. E. Fox, R. K. Curran, J. Chem. Phys. 34, 1595, (1961).
69. V. H. Dibeler, J. A. Walker, J. Chem. Phys. 44, 4405, (1966).
70. J. A. Simpson, C. E. Kuyatt, S. R. Mielczarek, J. Chem. Phys. 44, 4403, (1966).
71. C. A. McDowell, Trans. Fara. Soc. 50, 423, (1954).
72. R. D. Spratley, B.Sc. Thesis, University of British Columbia, (1961).
73. Venkateswarlu, J. Chem. Phys. 19, 293, (1951).
74. J. A. Cutler, J. Chem. Phys. 16, 136, (1948).
75. D. H. S. Mak, Ph.D. Thesis, University of British Columbia, (1966).
76. C. A. McDowell, J. W. Warren, Trans. Fara. Soc. 48, 1084, (1952).
77. D. C. Frost, C. A. McDowell, Unpublished results.
78. C. A. Coulson, "Valence", Oxford University press, (1961).
79. R. S. Mulliken, C. A. Rieke, W. G. Brown, J. Am. Chem. Soc. 63, 41, (1941).
80. L. Pauling, "The Nature of the Chemical Bond," Cornell University Press, (1960).